REPORT DOCUMENTATION PAGE

Form Approved OMB No. 0704-0188

1. AGENCY USE ONLY (Leave blank)	2. REPORT DATE	3. REPORT TYPE AND DATES COVERED
	December 1997	Final Report

4. TITLE AND SUBTITLE

The Concept For Creating Low Power Spaced Radar To Observe Small-Sized Debris Particles

5. FUNDING NUMBERS

F6170896W0293

6. AUTHOR(S)

Dr. Alexander Menshikov

7. PERFORMING ORGANIZATION NAME(S) AND ADDRESS(ES)

Vympel Corporation
3,4th 8 Marta Street
Moscow
Russia

8. PERFORMING ORGANIZATION REPORT NUMBER

N/A

9. SPONSORING/MONITORING AGENCY NAME(S) AND ADDRESS(ES)

EOARD
PSC 802 BOX 14
FPO 09499-0200

10. SPONSORING/MONITORING AGENCY REPORT NUMBER

SPC 96-4077

11. SUPPLEMENTARY NOTES

19980203 031

12a. DISTRIBUTION/AVAILABILITY STATEMENT

Approved for public release; distribution is unlimited.

A

13. ABSTRACT (Maximum 200 words)

This report results from a contract tasking Vympel Corporation as follows: Contractor shall develop a conceptual design for a low-power radar system capable of detection of millimeter particles from a space-based platform. The system shall be capable of long-term operation and shall be designed to detect particles of one millimeter or larger passing through an area of 40,000 square meters. A system architecture shall be provided that will demonstrate the technical feasibility of the system along with estimates of power and weight requirements.

14. SUBJECT TERMS

Electromagnetics, Space Debris

15. NUMBER OF PAGES

45

16. PRICE CODE

N/A

17. SECURITY CLASSIFICATION OF REPORT	18. SECURITY CLASSIFICATION OF THIS PAGE	19. SECURITY CLASSIFICATION OF ABSTRACT	20. LIMITATION OF ABSTRACT
UNCLASSIFIED	UNCLASSIFIED	UNCLASSIFIED	UL

THE CONCEPT OF CREATING LOW POWER SPACE BASED RADAR TO OBSERVE SMALL-SIZED DEBRIS PARTICLES

CONTENS

NOTATION.

S - the area of observed field,
λ- wavelength,
q - signal-to-noise ratio,
R - maximal range,
R_1 - minimal range,
σ- radar cross-section (RCS),
k - Boltzman's constant,
T - noise temperature,
F=T/290 K -relative noise temperature,
P_P - pulse power,
P - mean power,
τ- pulse duration,
E - energy in pulse,
f - pulse-repetition frequency,
$Q = 1/(f\tau)$,
A - antenna's area,
L - antenna's linear size ,
φ- the width of radiation pattern,
θ- scanning angle,
G - antenna's amplification coefficient,
V_0 - circular orbital velocity,
V - approach velocity,
η- coefficient of losses (the factor, taking into account reduction of signal/ noise ratio with respect to ideal radar due to power losses in transmitting and receiving tracts),

MMW - millimeter-wave band.

1. INTRODUCTION.

Distributions of space debris particles became the subject of the study due to requirements of spacecraft safety, especially the safety of manned missions. The aspiration to launch long-duration manned space missions in altitudes exceeding 500km is essentially deterred both by insufficient knowledge of the distributions of small-sized (1-100mm) debris and by the absence of clear enough concept for ensurance of manned missions safety.

The following three types of sensors are used to study space debris: ground-based radars, ground-based optical sensors, contact sensors on board of spacecraft.

Ground-based radars seem to be quite adequate for the posed task: they are capable to measure simultaneously three or even four (including Doppler velocity) parameters of object's motion, their capabilities slightly depend on the current status of troposphere, conditions of illumination by the Sun, position and phases of the Moon etc. However, ground-based radars must have very high energy characteristics in very high frequency bands: to observe 1-3mm particles we need a radar of short-wave millimeter band.

Optical ground-based sensors, having the advantages of simplicity and low cost are subjected to essential limitations, related to significant dependence on the status of the atmosphere and conditions of illumination and also with the need to perform lengthy observations of the particles to attain required accuracy of their tracks using only the measurements of two angular coordinates.

The main limitations of contact sensors are the low accuracy of determination of the tracks of contacting particles and the small areas of exposed surfaces, that make collisions too rare and the rate of the changes of particles' density may turn to exceed the rate of data collection.

Putting a sensor capable of remote measurements on board of a spacecraft allows to enlarge the size of field, observed from the satellite. A set of proposals for creation of on-board optical sensors arrived recently in Russia, USA and Japan. The idea of using on-board short-range radars, as far as we know, was first formulated by NASA (USA) [1] and became the subject of this study. In comparison with on-board optical sensors the radar has the advantage of the capability to perform measurements of three coordinates.

According to Ref.[1], the objective of this study is to develop the concept for creation of low-power radar system, capable to detect millimeter-sized particles from the space-based platform. The radar is to operate permanently during a long period of time, thus the requirements to power characteristics are the main subject of the study. Consumed power is to be as low as possible. The goal of the radar system is to detect orbiting debris of sizes 1mm and greater, which pass in the vicinity of the spacecrtaft. All the particles, passing through the area of 40000 sq. meters are to be detected. For example, if the radar's beam is observing the field of 45 degrees, millimeter particles are to be detected at the range of 295m, to obtain the total detection area of 40000 sq. meters. Arbitrary combination of angular field of view and detection range, providing total field of 40000 sq. meters, is acceptable. Assessments, made using modern space debris models demonstrate that in this way we can daily expect one detection of a particle, exceeding 1mm in size. The system is to determine the RCS of every detected object as well as its azimuth and elevation angle as functions of time.

The study will consider mainly the altitudes up to 1000km, where collision hazard, posed by debris particles to the space station, is most realistic.

The part 1 of this report was fulfilled in the main by specialist's of "Vympel", part 2 - by specialist's of "Radiophisika" .

PART 1.THE BASIS FOR THE REQUIREMENT TO THE ENERGY CHARACTERISTICS OF THE RADAR, THE SIZE OF ANTENNA AND THE FIELD OF VIEW

1 RELATIVE MOTION OF SPASE DEBRIS FRAGMENTS AND THE RADAR. ASSESSMENT OF EXPECTED FLUX OF OBSERVATIONS.

Adequate and rather simple (meaning minimal number of needed parameters) model of space debris in low Earth orbits can be designed under the following assumptions:

1) The orbits of debris particles are circular.

In fact the eccentricity of low orbits does not exceed several percent and vertical component of velocity does not influence the choice of parameters for the radar. In addition, due to atmospheric drag eccentricity decreases with time.

2) Longitudes of ascending nodes and initial positions of space debris fragments in their orbits are distributed uniformly.

Rationale for assuming such distribution are precession of the orbits and differences (even small) in altitudes. Refs. [2,3] derive and describe distribution of the density of debris fragments in spatial coordinates (altitudes, latitudes and longitudes) for this case:

$$(1.1)\quad N(r,\chi,\xi)=\begin{cases}\dfrac{N(r,i)}{2(\pi r)^2\sqrt{\sin^2 i-\sin^2\chi}}; & \sin^2 i>\sin^2\chi;\\ 0; & \sin^2 i\le\sin^2\chi,\end{cases}$$

where r - orbital radius, i - inclination, χ - latitude, ξ- longitude, N(r,i) -distribution function for the number of SD particles in orbital radius and inclination. Obviously, the distribution does not depend on ξ, variating from 0 to 2π.

Each spatial point, where the density is not equal to zero, is passed by two orbits with different longitudes of ascending node and with equal in magnitude but oppositely directed velocities. We can say that to every such point two components of SD particles with differently directed velocities are related. The density of both types of particles is two times less than the density, defined by (1.1). The density of each flux of SD are equal to the product of the density and the velocity vector, and if the point of observation is moving, than the multiplier is the relative velocity vector. The average number of particles, which pass through the field of observation, is equal to the integral of the density of the flux over the outer with respect to the approaching flux surface of the field S and in time along the track of the radar.

In general the result depends on the orbit of the spacecraft-carrier of the radar, on the shape, sizes and position of the field of view with respect to the center of the carrier. However, when the dimensions of the field are small with respect to the altitude, for greater part of the range of orbital inclinations the density of the flux practically does not variate within the field of view and slightly differs from the density of the flux in the orbit of the carrier. Thus it is sufficient to consider the case when conditional center of the field of view coincides with orbital position of the center of the carrier and use the results of calculations also for the case when the center of the field of view does not coincide with the center of the carrier.

The cases when $i+i_0=\pi$ (i_0 - orbital inclination of the carrier), present an exception, when SD particles and the radar are moving in identical tracks in opposite directions. For example, when $i = 0$, $i_0 = \pi$ and equal altitudes of the orbits of the particle and the platform, each particle collides with the platform twice per revolution. These specific cases are not of practical interest (since they constitute a set of zero measure) and won't be considered . The formulas of the calculations are presented in the Appendix and the results are discussed further.

Table 1.1 presents the results of computations for the ranges of approach velocities V and the absolute value of approach angle γ (in the radar's carrier coordinate system) for various inclinations of carrier's orbit and space debris particles. The orbit of the platform is considered circular with altitude 500 km. The extreme point of theranges correspond to the equator. The table also presents the values for the number of intersections of the field with the area 1 sq.km by SD particles per day NuS. The scale is chosen assuming the condition that 1 km in altitude contains 1000 fragments. Illustrations of fig. 1.1 present V (left chart), γ (right chart) and the number of intersections (lower chart) as functions of the eccentric anomaly angle for the quarter of a revolution, starting from the ascending node (then the pattern is repeated first in reverse order, then in direct order and again in reverse). The number of intersections are normalized to the unit for a quarter of revolution.

Table 1.1

$i_0 = 1^0$				$i_0 = 30^0$			
i (deg)	V (km/s)	γ (deg)	NuS	i (deg)	V (km/s)	γ (deg)	NuS
2	0.27	87	0.68	0	4.0	75	0.65
30	4.0	75	0.70	31	0 - 7.8	60-90	0.78
60	7.7	60	0.79	60	4 - 11	45 - 75	0.89
90	10.5	45	0.97	90	7.8-13.2	30 - 60	1.1
120	13.3	30	1.39	120	11-14.6	15-75	1.65

$i_0 = 60^0$				$i_0 = 85^0$			
i (deg)	V (km/s)	γ (deg)	NuS	i (deg)	V (km/s)	γ (deg)	NuS
0	7.5	60	0.75	0	10	47	0.85
30	4-10.7	45-75	0.80	30	7-12.7	32-63	0.89
61	6-13.2	30-90	1.25	60	3.3-14.2	18-77	0.97
90	4-14.3	15-75	1.68	90	0.7-15	3 - 85	7.29
121	7.5-13	0-60	4.33	120	4.3-14.8	13-73	1.0

$i_0 = 120^0$			
i (deg)	V (km/s)	γ (deg)	NuS
0	15.1	30	1.25
30	10.7-14.5	15-45	1.45
61	7.3-15	0-60	4.46
90	3.8-14.6	15-75	1.60
120	0-13	30-90	1.20

One can see from the table that the input of orbits with different inclinations to the expected number of particles is different: this input is as greater as the motion of the particles is more close to the motion, opposing the motion of the platform. Mention, that greater velocities correspond to small values of γ, and V=0 corresponds to $\gamma = \pi/2$.

Real distribution of small-sized particles in inclination is unknown and may alter with time due to drift in altitude, new satellite break-ups etc. For cataloged objects distribution in inclination are presented in Refs. [3,4,5]. According to these data, approximately one half of the objects have inclinations within 80 - 100 degrees, 85% - within the range of 60-100 degrees and approximately 15% - within the range of 20 - 40 degrees. Fig.1.2 depicts the

hA/hP= 500/ 500; i0= 60

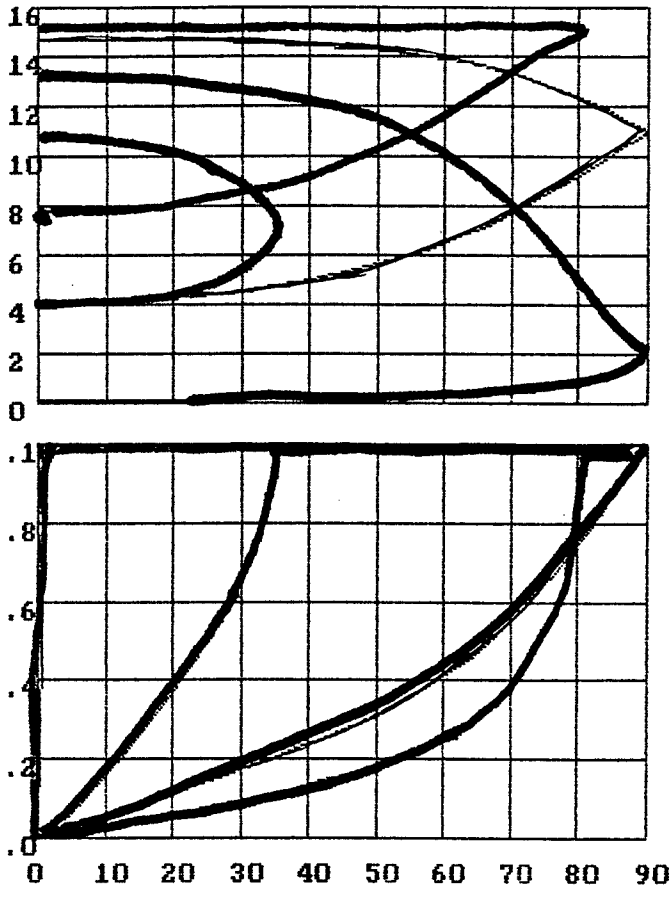

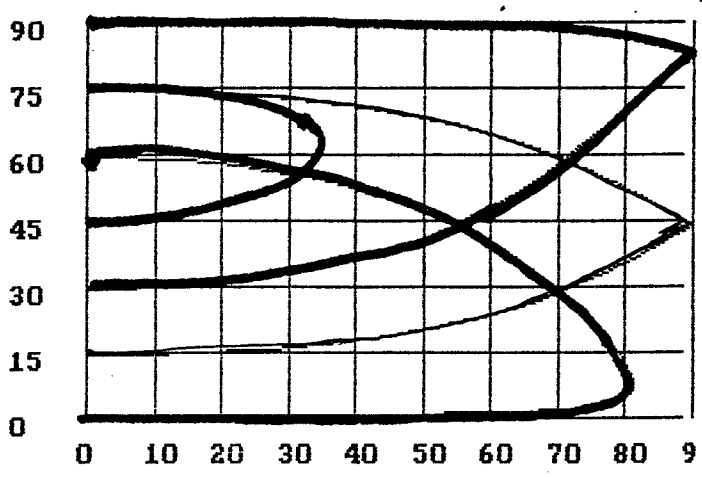

i= 1 -green; NuS= 0.263
i= 30 -cayn; NuS= 0.291
i= 61 -red; NuS= 0.458
i= 91 -magent; NuS= 0.614
i=121 -brown; NuS= 1.580

hA/hP= 500/ 500; i0= 85

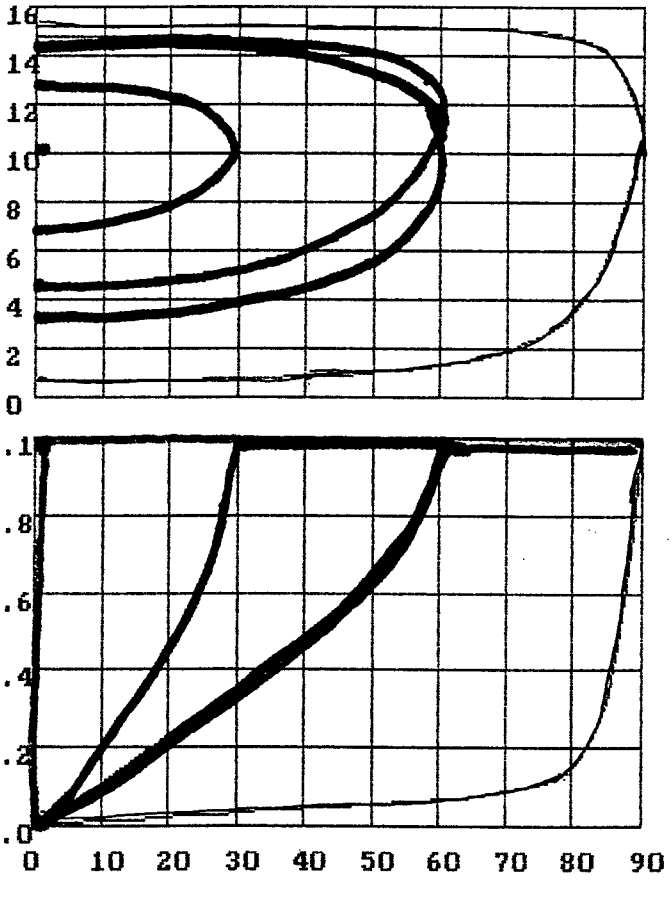

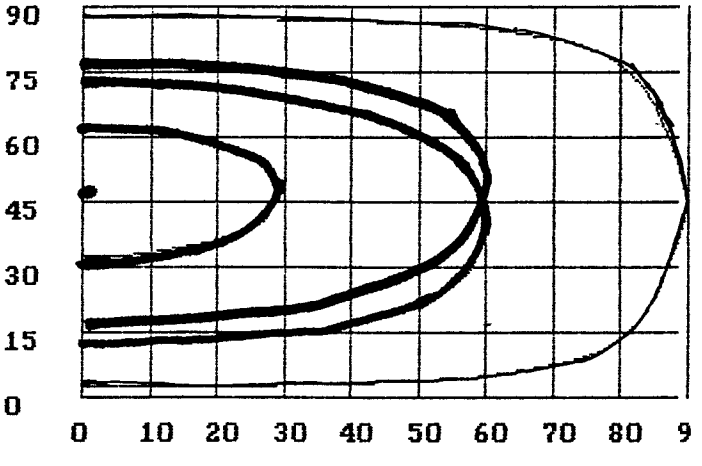

i= 1 -green; NuS= 0.309
i= 30 -cayn; NuS= 0.325
i= 60 -red; NuS= 0.323
i= 90 -magent; NuS= 2.662
i=120 -brown; NuS= 0.365

Fig. 1.1.

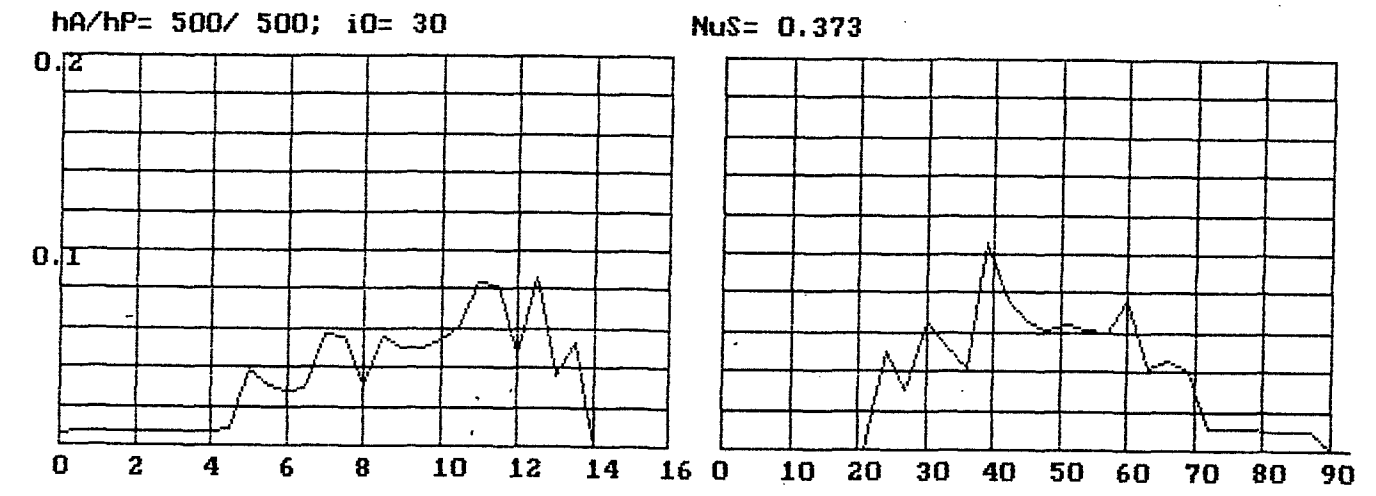
hA/hP= 500/ 500; iO= 30
NuS= 0.373
0.2
0.1
0 2 4 6 8 10 12 14 16
0 10 20 30 40 50 60 70 80 90

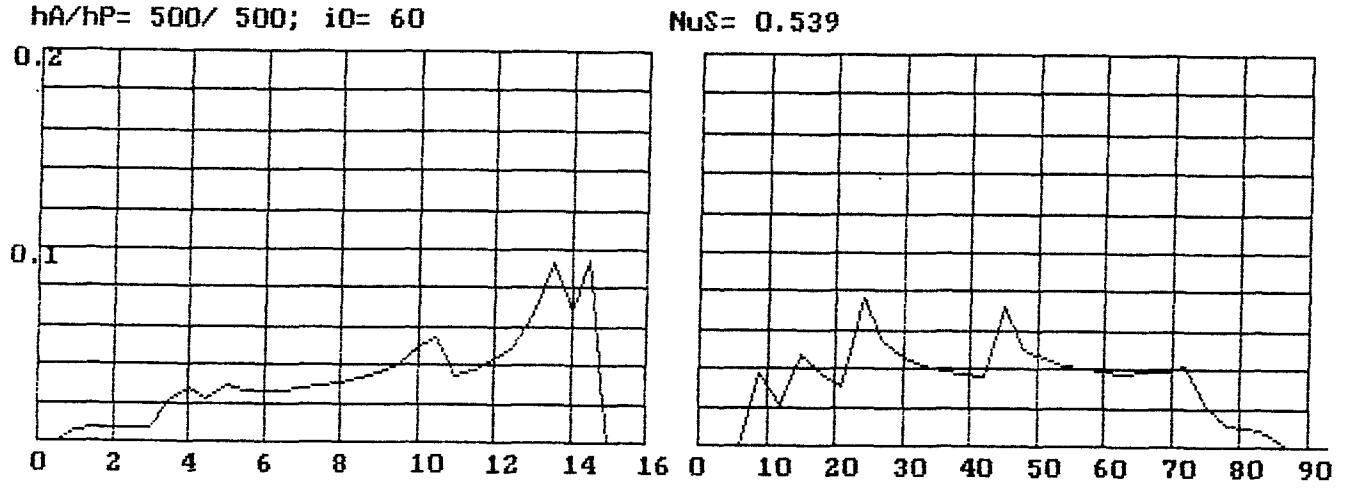
hA/hP= 500/ 500; iO= 60
NuS= 0.539
0.2
0.1
0 2 4 6 8 10 12 14 16
0 10 20 30 40 50 60 70 80 90

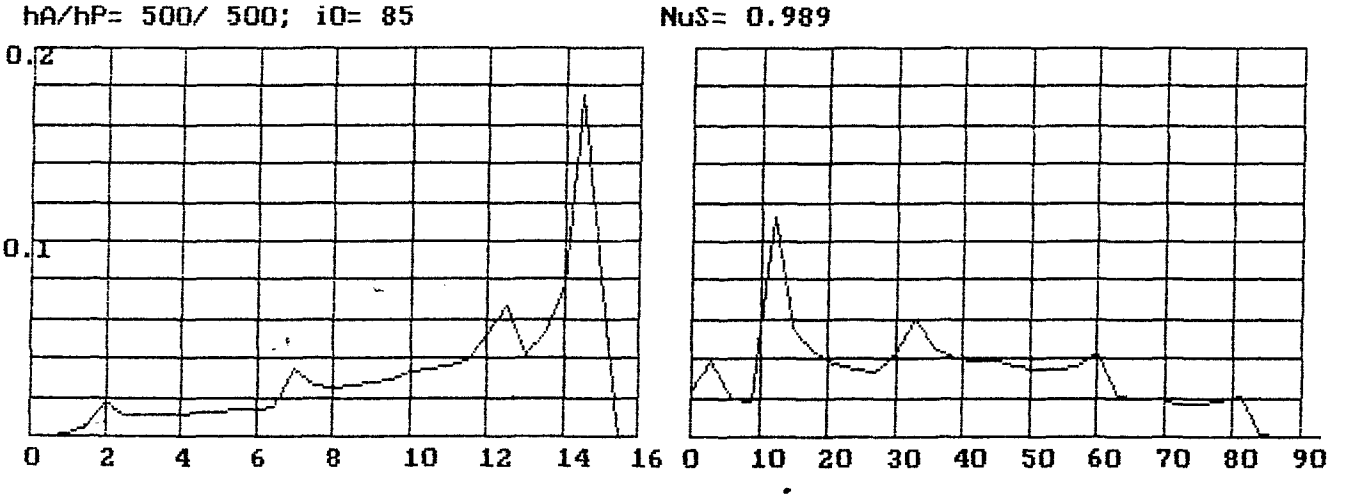
hA/hP= 500/ 500; iO= 85
NuS= 0.989
0.2
0.1
0 2 4 6 8 10 12 14 16
0 10 20 30 40 50 60 70 80 90

Fig. 1.2.

distribution for velocity V and the angle γ, obtained by summing the distributions with i =30,70,85 and 100 deg. with the weight coefficients 0.15,0.35,0.25 and 0.25 respectively, for various inclinations of carrier's orbit. These distributions do not significantly differ from those obtained for corresponding inclinations on the basis of real satellite catalog Ref. [4].

Table 1.2 presents the values of NuS for various i_0, averaged using the same weight coefficients. It follows from these data that the choice of carrier's inclination within the range of 70-110 deg. can be considered rather favorable.

Table 1.2

i_0(deg)	30	50	60	70	75	85	95	100	110
NuS	1.05	1.25	1.48	1.96	2.30	2.71	3.60	2.54	3.09

Evaluation of the expected number of observations will be obtained using assessment of the number of SD particles with sizes exceeding 1mm - 3 10^7 ., presented in Ref.[5]. If these SD particles are distributed within the range of 500 km, then for 1 km we will have 6 10^4 fragments and the expected number of observations for the inclination of carrier's orbit 70^0 will be equal to 120 per day for 1 km^2 of the field of observation (5 for 40000 m^2).

Above we considered that the center of the field of observations coincide with the center (of weight) of the carrier. Characteristics, treated above were not influenced by slight displacement of the center of the field with respect to the orbit. However, certain useful effect of shifting the center of the field in altitude, does exist.

In case the field of observations is located in the same altitude as the center of carrier, then due to equality between orbital periods of the carrier and SD particles one and the same particles will be observed repeatingly from revolution to revolution. This periodicity will be affected only by differences in atmospheric drag and precession rates due to difference in inclinations. A shift of observations' field in altitude will result in the difference of orbital periods of the field and the entering particles, thus in consequently repeating after half of revolution approaches between the orbits, the field will be entered by different parts of fragments' orbits. The shift in horizontal plane in the direction, normal to velocity of the carrier for half a revolution is equal to

$$\Delta L=(3\pi/2)\Delta h \sin \gamma_1,$$

where Δh - difference in altitudes, γ_1 - the angle of orbits' intersection in not-moving coordinate system (reckoned from direction of opposing motion) It is sufficient that this shift to exceeds dimensions of the field.

Since the particles with enter the rather small field of view of the radar rather seldom (several events per day), the observation is to be rather lengthy to acquire statistically valid results. Therefore, for the observations we must choose the altitude band, where the distributions of the particles are do not vary too quickly due to transition of particles to lower altitudes, caused by atmospheric drag. The table presents the calculated values for the decline of circular orbit altitude for the aluminum sphere (for two values of its diameter and two initial altitudes). The altitude distribution of the atmospheric density correspond to the average level of solar activity.

Table 1.3

height	300 km		400 km		500 km		600 km	
diameter	1 cm	1mm	1 cm	1 mm	1 cm	1 mm	1 cm	1 mm
velocity of lowering	4.4 km/day	44 km/day	440 m/day	4.4 km/day	88 m/day	880 m/day	30 m/day	300 m/day

To have the RMS error for the estimation of the number of particles within certain spatial domain not exceeding 20% of the mean, the mean value must not be less than 25. Assuming, that the average number of registered particles will be 5 per day, we will have to perform the observations during 5 days to attain the required accuracy of 20% (regarding the considered observed altitude band ≈5km). In case in addition we need to evaluate the distribution of particles in inclination, then for the range of inclinations into 5 intervals and the distribution in inclination close to uniform, 25 days of observations are required. For the stationary distribution of particles, when their amount in high altitudes is being permanently replenished, this is insignificant. However, when we pose the task to register the bursts of particles' flux, the factor of particles' altitude decline will limit the minimal size of the particles and the minimal altitude of the radar. For the minimal size of 1 mm the altitude of the radar must be not lower than 600-700 km, for sizes 3-5 mm - 500 km. For the acquisition of altitude and inclination distributions of particles several (4-6) radars will be required, distanced in altitude within the range, where significant amount of particles is expected (500- 900 km). The altitude bands, controlled by different radars, unfortunately, will not overlap, and one will have to extrapolate the results of the observations. Nether the less, such system will be essentially more informative than the system, based on contact sensors, installed at the same satellites. Further enhancement of efficiency, apparently, can be attained using combination of radar and optical sensors on board of satellite platform.

2 ANALYSIS OF THE VARIANTS OF THE SHAPE OF RADAR'S FIELD OF VIEW AND THE EVALUATION OF MOTION PARAMETERS OF DETECTED TARGETS.

We mentioned above that specific feature of the task is the condition that the directions of targets' (SD particles) approach rather slightly (not more than 2-4 %) deviate from the horizontal plane, have significant spread in azimuth γ (from -90^0 to $+90^0$) and their value varieties as $\cos\gamma$. Distribution of particles' flux in approach angles declines to zero by the boundaries of the range (fig. 1.2).

Great angular velocities of the particles exclude the possibility to use mechanical scanning, and the requirement to determine coordinates as function of time - the possibility to use single-beam antenna without control of the beam. Two possibilities remain: phased array and non-scanning antenna with mono-pulse pelengation. We will see further, that the latter can be considered as extreme case. Thus we will assume that the radar is equipped with antenna with as narrow as possible (for the sake of simplicity and low cost) scanning sector Θ. This is to be sufficient to produce the field of detection with required area and to provide determination of parameters of particles' tracks. Since requirements to the accuracy of parameters' determination are not posed (Ref. [1] requires to determine RCS of each detected object as well as the range, elevation angle and azimuth as functions of time) the assessment of acceptability of accuracy characteristics will be based on experience of the investigators.

It is expedient to compare two variants of the orientation of the scanning sector: along direction of the motion - variant «L», and across this direction - variant «C». In the latter case vertical orientation of the sector is preferable: first, thus repeated observations of one and the same particles is excluded (see the end of the previous section), second, in this case the range of radial velocities, defining the requirements to the number of receiving channels and essentially influencing the choice of the probing signal, is essentially narrower. The width of this range is approximately $\pm(e + e_0)V_0$, where e, e_0 - orbital eccentricities of the platform and the target, i.e. is not greater than ± 0.75 km/s for low orbits, and for the variant «L» this range spreads from 0 to 15 km/s (for the center of the sector).

The most economical mode of detecting the targets, passing through the field of view, is the scanning of the boundary fences. The width of the fences and the scanning rate are to be great enough to provide that the target will be illuminated not less than n times in course of the

time of its crossing the fence. The value of n is determined by the employed detection criteria and the algorithm for determination of coordinates and velocities.

The fence is to be rather densely covered by the beams of transmitting antenna, configured in the shape of one or more "lines". One can easily see that the choice of the number of the lines does not influence the requirement to the duration of scanning one line - T_0 :

(1.2) $T_0 = m\,\Phi/(\varphi\, f) < \varphi\, R_1/(nV_c)$,

where Φ - the length of the fence, φ - the width of the beam (is equal to the width of the line), R_1 - minimal range, V_c - the component of the target's velocity, directed across the fence, m - reserve coefficient for overlapping of the beams (approximately 1.5 - 2), n – the number of scanning cycles, needed for detection of the target with required probability, f - signals' repetition frequency (f is connected with maximal range R: $f = c(Q-1)/(2QR)$, $Q = 1/(f\tau)$, τ - pulse duration, c - velocity of light. It follows from (1.2) that the shape of the fence is to be chosen according to the minimum of the value of ΦV_c within the range of directions of targets' approaches. The cross-section area of the observations' field is to meet the requirements of the terms of reference.

When $m\,\Phi/\varphi$ is less than 10, discrete character of the number of beams, covering the fence, becomes significant. For this number from (1.2) we obtain the inequality

(1.2') $M^2 \le m/n\ \Phi\, f R_1/(2V_c)$.

Since Φ is dependent on the width of the scanning sector, we can choose the latter so that the inequality (1.2') transfers to equality. Further we will consider this condition satisfied.

Comparison of the variants of configuration of the fences for further considerations were chosen: for variant «L» - two plane fences, depicted in fig.1.3, which intercepts the targets, entering the field from the front as well as from the side, and for variant «C» - three subvariants (fig.1.3): «C1» with plane fence, normal to the motion of the radar, «C2» with the fence in the shape of half of circular cone and «C3» with the fence in the shape of bihedral angle, based on two sides of equal-sided triangle. In the first case the fence is most short, but the intersection velocity reaches its maximum and the overlapped area subsides to zero for of greater values of approach angles. In the second case the second of the mentioned limitations does not exist (to be more precise, is not so marked), and for the third case even the first limitation is removed (as far as possible). The fences are inscribed to the circle with radius, equal to the value of the maximal deviation of the beam from the normal to antenna's aperture, as it is depicted in chart 1.3b.

Comparison of scanning patterns in energy characteristics.

For comparison of energy characteristics the following parameters are essential: the covered area of particles' flux S, maximal velocity of crossing the fence $\max V_c$ and the length of the fence Φ. We would like to have S slightly dependent on the approach angle, within the range of the angles where the density of the flux is not zero, and the product $V_c.\Phi$ is minimal.

To characterize the function $S(\gamma)$ numerically, we will introduce the mean $\langle S \rangle$, resulting from approximation of the angular distribution of the flux by the function $\cos\gamma$, corresponding to the way the flux subsides to zero by the boundary of the range.

For variant «L»

(1.3) $S(0)=\sin^2(\Theta/2)(R^2 - R_1^2)$, $S(\pi/2) = \sin(\Theta/2)(1-\sin^2(\Theta/2))\,(R^2 - R_1^2)$.

Equating these values to reduce dependence of S on the azimuth,

we obtain $\Theta \approx 1.25$ rad. and

$$\langle S \rangle \approx 0.35 (R^2 - R_1^2).$$

For variant «C»

(1.3') $$S(\gamma) = U(\gamma) \cdot \Theta(R^2 - R_1^2)/2,$$

where $U((\gamma) = \cos \gamma$ for «C1», $U((\gamma)=(1+\cos \gamma)/2$ for «C2» and $0.375<U((\gamma)<0.43$ for «C3». For the sake of uniformity it will be convenient to present the area as function of angle in the same manner for variant «L» also, though Θ is of certain value (1.25 rad) for this case.

Parameters of the variants are presented in table 1.4.

Table 1.4

Variant	«L»	«C1»	«C2»	«C3»
<U>	≈ 0.56	0.78	0.89	0.8
$\max V_c/V_0$	1.42	2	2	1.5
Φ/Θ	1.33	1	1.57	1.73

Relationships (1.2), (1.3) allows to connect the energy characteristics of the radar with the parameters of the field of view. One can see that it is not energetically profitable to be adherent to too small values of minimal range R_1 : we will have to widen the fence and "spread" the power over the large sector. We have an optimum for R_1, which value depends on the minimized energy parameter.

In case the area of receiving antenna A can be chosen to have the receiving beam narrower than the transmitting one, and the beam, produced for transmission can be covered by any required number of receiving beams, then the single energy parameter, influencing signal/noise ratio is the value $\Pi = \eta PA/F$, where η - coefficient of total losses (of the tracts of transmitter and receiver, of the antenna and within the signal processing system), P - average power of the transmitter, F - normalized (divided by 290 K) noise temperature of receiving system.

It is easier to realize a a radar with co-located receiving-transmitting antenna and with equal widths of transmitting and receiving beams. In this case transmitting beam is covered by a set of 4-7 receiving beams to reduce energy losses to form pelengation characteristics. Then the area A is determined by the relationship

(1.4) $$A=0.8 (\lambda/\varphi)^2 = 0.4 \cdot \lambda^2 c R_1/R (Q-1)/(Q mn V_c \Theta),$$

and signal/noise ratio is determined by the value $\eta P/F$. Finally, under appropriate limitations for the transmitter, minimization of the energy of the pulse E may be of interest.

Using the main equation of radar location and the relationships, presented above we will have the following formulae for the three energy parameters, mentioned earlier:

(1.5) $$\Pi = \eta \frac{PA}{F} = \alpha_1 mnq \cdot \frac{V_0 S^{3/2}}{\sigma} \cdot \frac{x^4}{(x^2-1)^{3/2}} 10^{-18} \text{ w} \cdot \text{m}^2;$$

(1.6) $$\eta \frac{P}{F} = \alpha_2 (mn)^2 q \frac{V_0^2 S^{3/2}}{c\sigma\lambda^2} \cdot \frac{Q}{Q-1} \cdot \frac{x^5}{(x^2-1)^{3/2}} 10^{-18} \text{ w};$$

(1.7) $$\eta \frac{E}{F} = \alpha_3 (mn)^2 q \frac{V_0^2 S^2}{c^2 \sigma \lambda^2} \cdot \frac{Q^2}{(Q-1)^2} \cdot \frac{x^6}{(x^2-1)^2} 10^{-17} \text{ j},$$

where $x=R/R_1$, α_1 , α_2 , α_3 - the coefficients, which values for «L» and «C» variants are given in table 1.5. Comparison of the variants with regard to corresponding energy criteria thus means comparison of the values of α_1 , α_2 , α_3.

Table 1.5

Variant	α_1	α_2	α_3
" L "	0.64	3.02	9.6
" C1 "	$0.41\ \Theta^{-1/2}$	$2.06\ \sqrt{\Theta}$	5.6
" C2 "	$0.53\ \Theta^{-1/2}$	$4.17\ \sqrt{\Theta}$	10.1
" C3 "	$0.51\ \Theta^{-1/2}$	$3.35\ \sqrt{\Theta}$	8.9

Mention the character of their dependence on the size of the field of view Θ for variant «C»: required value $\Pi=\eta PA/F$ decreases with widening of the sector as $\Theta^{-1/2}$, required mean power increases as $\Theta^{1/2}$, and required pulse energy does not depend on Θ. It means that the choice of Θ can be completely used to minimize potential Π or the power.

In these relationships we have minimum in x corresponding to x=2 for Π, to x= 1.58 for average power and for x= 1.73 for the energy. The power increases rather slowly with deviation from the minimum (variation of x from 1.58 to 1.73 corresponds to 2% increase and from 1.73 to 2 - to 12% increase). Thus for further evaluations we shall take x=1.73.

For fixed x maximal range and the scanning sector are interrelated and any of these values can be used as primary parameter.

It should be taken into account that the increase of Θ provides the possibility to increase the time of observation and increase the accuracy of measuring particles' velocity components. Thus, in case the possibility). to create low cost multi-beam receiving antenna existed, preferable choice would be the wide sector for variant «C». However, for the system with equal beams for transmission and receiving, the energy advantages of the narrow-field system are obvious. With regard to energy characteristics, the best of the subvariants is «C1».

Table 1.6 presents the results of calculating parameters φ, R, R_1 for variants «L» and «C» for various sizes of the sector Θ and for S=40 000 m^2, x=1.73, m=1.5, n=2 (about n see next paragraph).

The last line of the table gives the number of the beams M, covering the fence - $M = [m\cdot\Phi/\varphi]+1$, where the brackets mean taking enter value in defect.

Diminution of Θ to the limit (for $\Phi/\varphi \sim 1$) leads to single-beam (for transmission) radar without search. In this case the minimum of $\eta P/F$ in R_1 becomes more abrupt for small ranges. Parameters for this case are given in the last column of table 1.5 (since the tracking of the detected target is not assumed, n is taken equal to 3). This case is not of interest, since the resulting sizes of antenna are too great (tens of meters for mm-band) and the accuracy of motion characteristics' determination - too low.

Table 1.6

	"L"	"C1"	"C1"	"C2"	"C2"	"C3"	"C3"	
Θ(deg)	71.7	5	1	5	1	5	1	Θ=φ
φ (deg)	1.42	0.39	0.18	0.49	0.22	0.45	0.2	0.01
R_1(km)	0.24	1.08	2.4	1.0	2.25	1.08	2.4	40.8
R(km)	0.42	1.88	4.2	1.76	3.93	1.88	4.2	46.0
M	100	20	9	24	11	29	13	1

The increase of range under the same sector of scanning or the increase of the sector under the same range will result in the increase of the area of the observed field.

Evaluation of targets' motion parameters: comparison of possible variants.

To determine the orbit we need three components of initial position of the particle and three components of velocity vector. Knowing initial position and velocity of the particle we can determine its orbital inclination i, argument of latitude u, eccentricity e and argument of perigee u_p, using, for example, the following system of equations:

$$\cos i = F_1 \cos i_0 - F_2 \sin i_0 \cos u_0;$$
$$\sin i \cos u = F_1 \sin i_0 \cos u_0 + F_2 \cos i_0 ;$$
$$\sin i \sin u = \sin i_0 \sin u_0;$$
$$e^2 = [(V_g / V_0)^2 - 1]^2 + (V_g \cdot V_v / V_0^2)^2;$$
$$\tan (u-u_p) = V_g \cdot V_v / (V_g^2 - V_0^2),$$

where V_g, V_v - horizontal and vertical components of particle's velocity with respect to the Earth (the orbit of the radar is considered to be known precisely), V_0 - circular velocity in altitude of detection, i_0 , u_0 - radar's inclination and argument of latitude, F_1 , F_2 - functions of the absolute value and the direction of the measured velocity vector. For small orbital eccentricities of the radar and the particle these functions may be represented as cos 2γ and 2tan γ, where γ - the angle of particle's approach.

The task of determination of particle's position for the moment of detection is not critical: for quite achievable parameters of the radar and calculated above ranges it can be determined with acceptable accuracy- units of meters (we consider the errors in range not to exceed the errors in cross coordinates). The critical task is determination of velocity.

Analysis can show that the relative motion of the particles with respect to the radar within the field of view with dimensions up to 10 km can be considered to be uniform motion in straight lines - acceleration does not exceed 0.05 m/s^2. Thus follows, that it is not possible to update one components of the velocity by more accurate measurements of the other ones (for example, radial velocity) using equations of motion. Generally speaking, we need to measure all three components.

The task is simplified in case the orbits of the particles can be considered circular. Here the radial (with respect to the Earth) component of velocity is equal to zero and the magnitude of tangential component is determined by the altitude, i.e. by initial position of the particle. We

have to determine orbital inclination and longitude of ascending node, which are determined by approach angle in horizontal plane and the moment of detection.

Thus, the approach angle is the most important parameter to be measured. Then follows the values of vertical and horizontal components of velocity, allowing to determine the eccentricity and perigee argument.

For measurements of approach angle in all the variants essential are the cross components of velocity, which can be calculated using increments of the angles. We need to obtain measurements of angular positions of the target for the most long temporal (to be more precise, angular) base: root-mean-square (RMS) error in velocity is inversely proportional to the width of the sector between boundary measurements of the angle.

To combine this condition with quite natural aspiration to simplify the antenna, it is desirable to have the measurements at the entrance of the scanning sector and at the exit. From this point of view advantageous is the system with semi-circular fence, bordering the sector (variant"C2"). It is essential, that on the basis of measurements of the angles of target's entering and exit from the circular zone, the approach angle is determined with RMS error, not depending on the approach angle and "aiming" distance (the distance to the center of the zone) and equal to

$$\sigma_\gamma = \sqrt{2}\,\sigma_\alpha / \Theta = \sqrt{2}\,a\varphi / \Theta \ ,$$

where a - coefficient of proportionality between angular RMS error and the width of the beam. To evaluate the distribution of particles in inclination, when the range of inclinations is divided by 5 intervals and the distribution in inclination close to uniform, RMS≤0.15 rad. is required. To obtain the error $\sigma_\gamma \le 0.15$ rad. for a = 1/6, that corresponds to noise error for q=20, it is sufficient to have $\Theta / \varphi \ge 2$.

For variants "C1" and "C3" the error σ_γ of measuring the approach angle using the points of intersecting the fence (first mark) and the ring of maximal deviation of the beam (second mark) unlimitedly increases with approach to the angles, formed by intersection of the fence with the ring of the beam. Thus the field of view won't be used completely and its size must be chosen with certain reserve. In fact, this situation practically reduces to zero energy advantages of these variants for the scanning mode.

Taking intermediate measurements will certainly allow to reduce the noise error. However, the possibility of arrival of "non-smoothable" (slowly evaluating) errors makes the hopes to reduce the errors more than twice not very realistic.

The fulfilled analysis revealed that the preferable variant of the field of view is the variant with scanning of vertically located semi-circular fence, its convexity oriented along direction of radar's motion. The possibility to handle the beam within the ring must be provided. Nevertheless, further we will also consider variant "C1" as the most economical in power.

3. ASSESSMENT OF REQUIRED ENERGY CHARACTERISTICS OF THE RADAR.

3.1 The probability of track's detection and false alarms

We start with determination of the number of scanning cycles, needed to detect the target with required probability. Since the required power is proportional to qn^2, and q changes as function of n rather slowly, n is to be minimal. Choosing n=1 would result in the need to increase the detection threshold up to hardly controlled value (in radar technique practice usually the tuning of the noise threshold on the basis of the frequency of its surpasses). For n=2

and detection criterion "1 of 2" it is sufficient (it will be demonstrated further, treating the issue of false alarms with account of tracks' selection) to put the probability of false alarm within one resolution element equal to 10^{-5} . This false alarm probability and probability of detection in single measurement equal to 0.9 (0.99 in two circles) correspond to threshold value of signal/noise ratio $q \approx 20$.

The task of selecting the false marks (surpasses of the noise threshold) is closely related to the task of determination of parameters of the track. The practice revealed that most efficient is selection of the tracks. Assuming this efficiency we soften the criterion of primary detection and reduce the requirements to radar's energetics. Let us evaluate the number of track's confirmations needed to attain acceptable level of false tracks.

The frequency of false marks is equal to

$$\omega = \frac{F}{\tau}\left(1-\frac{R_1}{R}\right),$$

where F - probability of false alarm within the resolution element τ - duration of resolution interval in signal's delay. For $F=10^{-5}$, $\tau = 0.5$ μs, $R/R_1 = 1.73$ we have $\omega = 8.4$ 1/s. Assume, according to the previous section, that after the first mark within the fence is acquired, the fence moves in the manner, ensuring the capture of the target on its exit out of the sector; and that the decision of a track detection is made on the basis of two marks - one within the fence and the second on the outlet of the sector. Then the first false mark can be confirmed by false mark from arbitrary point of the ring, located more distant from the front border of the ring, than the first one, but within determined for each point temporal interval (equal to the interval of passing through the beam - two pulses), since approach velocity is definitively connected with approach angle. Thus the frequency of arriving pairs of false marks, forming a track , is equal to:

$$\omega_2 \approx 2F\omega J,$$

where J - the number of cells within the domain of uncertainty of readings of the mark's position for all the coordinates - range, angle and time ($J \approx 100$). Evidently, this frequency is too great and more strict criteria for detection of the a track is needed.

For detection on the basis of three marks it is expedient to obtain the first confirmation at least by one of the two pulses within a short interval after detection in the fence- immediately after the scanning circle, and the second one - at the outlet of the sector. The frequency of arrival triplets of false marks, forming a track, is equal to

$$\omega_3 \approx 4F^2\omega J \approx 0.02 \text{ 1/ day}.$$

This frequency can be considered acceptable.

The probability of track's detection (for the probability of obtaining a mark within the fence -0.99) will be not less than 0.97.

Consume of power for tracking the targets, detected in the fence can be considered insignificant, since their expected number is small (units per day) and the time of residence within the sector is of the order of 0.1 sec. or less. Thus it is acceptable even to interrupt the scanning for the time while detected target is passing through the sector. No principal difficulties exist here. Details of the algorithm can be chosen after the architecture of the radar, characteristics of the beam control and computer hardware will be determined.

3.2 The choice of wavelength band.

Under the condition, that the main requirement to the radar is to make the consumed power as small as possible, the wavelength band is to be chosen to ensure the maximum product of transmitter's efficiency, the wavelength squared and target's RCS (see (1.6,1.7)). In fact thus follows that the wavelength is to be chosen close to the upper limit of the resonance

domain for particles of minimal size. For particles with sizes 1 mm this condition is satisfied for the band 95 GHz (3,2mm).

Let us evaluate the minimal RCS of the particle, which will be refereed to in energy assessments. We will assume that small particles can be considered (with regard to scattering surface) to be spheres. This assumption is rather strong and can be based on the following considerations: for particles of 1mm size, which determine requirements to energy characteristics of the radar, RCS within the treated band is to be slightly dependent on the aspect of observation, i.e. slightly deviate from the sphere with regard to the character of this function. For large particles such representation is unacceptable, but they are not the sort of particles which poses requirements to energy characteristics of the radar.

From dependence RCS of a sphere as function of its size [6] one can see, that for the band 95GHz the minimal scattering surface is realized for the particle approximately 2 mm in diameter and is equal to 1 mm^2. This will be the reference RCS value further.

3.3 Assessment of required energy characteristics of the radar.

Now , for chosen wavelength and target's RCS we shall evaluate the required transmitter's power using the formulas (1.6), (1.7) for variant "C1" and "C2" and the following values of parameters:

$S = 40000\ m^2$, $V_0 = 7.9$ km/s, $R/R_1 = 1.73$, $q = 20$, $Q >> 1$, $m = 1.5$, $n = 2$, $\lambda = 3.2$ mm. Thus we have the result:

for variant "C1" $\eta E/F = 1.\ 1\ 10^{-3}$ J,

for variant "C2" $\eta E/F = 2.\ 1\ 10^{-3}$ J.

In our calculations of power we will consider a discrete set of possible number of beams within the fence M. For each value of M first we determine the width of the scanning sector using formula (1.2') , then using formulas (1.2), (1.3') - the width of the beam and maximal range, according to $L = \lambda / \varphi$ - diameter of the antenna, from the relationship $P = E f = 1.5\ 10^5 E / R$ (km) - the average power. For coefficient of losses we will take 0.1, for noise temperature of receiving system - 200 K (see Part 2). Results are presented in table 1.7 for "C1" and in table 1.8 for "C2".

Table 1.7

M	Θ (deg)	φ (mrad)	L(m)	Θ / φ	R(km)	P (w)
8	0.59	2.26	1.41	4.5	3.85	300
7	0.45	2.0	1.6	3.9	4.4	260
6	0.34	1.7	1.9	3.5	5.1	220
5	0.23	1.43	2.24	2.8	6.17	190
4	0.14	1.09	2.93	2.24	7.9	140
3	0.08	0.84	3.8	1.66	10.46	110

Table 1.8

M	Θ (deg)	φ (mrad)	L(m)	Θ / φ	R(km)	P (w)
8	0.38	2.26	1.41	2.9	4.5	470
7	0.3	2.0	1.6	2.6	5.1	420
6	0.21	1.7	1.9	2.15	6.1	350
5	0.15	1.43	2.24	1.83	7.1	300
4	0.1	1.13	2.8	1.51	8.8	240
3	0.056	0.9	3.5	1.08	11.7	180

One can see from the tables that the conditions of acceptable accuracy of the measurements of motion direction ($\Theta / \varphi \geq 2$), acceptable size of the antenna (L approx. 2 m) under minimal power are satisfied for the lines with M equal 5 for both variants. The required power for variant "C2" is 1.6 times greater in this case.

CONCLUSION

The posed task of creating low-power space-based radar, capable to detect and determine the tracks and RCS of space debris particles with sizes as small as 1mm, can be solved under the average radiated power of 150-250 w.

Preferable band (among the developed ones) is the band 94 GHz.

The radar can have co-located transmitting and receiving antenna. Diameter of the antenna is - near 2 m, the scanning sector - $0.15\text{-}0.2^0$.

For the required area of the detection zone equal to 40000 m^2 maximal range of the radar is to be 6-7 km. Minimal range, for which not less than twice illumination of the target during its pass through the fence (the width of the fence is equal to the width of the beam) will be provided is - 3.5-4 km.

The scanning sector is to be posed across the motion of the platform in vertical direction preferably. The best variant of the beam control is assumed to be the cyclical scanning of the fence, shaped as a semi-ring, bordering the scanning sector from the front (in the direction of motion) with the transfer to the mode of updating the track after the detection of the target within the fence.

The accuracy of target's position determination will be of the order of several meters. Accuracy of determining the direction of the relative motion in the horizontal plane is 10^0. Accuracy of determining the vertical component of the velocity- 200 - 300 m/s.

References to part 1

1. .Statement of Work for Vympel Corporanion, NASA, 11-01-1995.

2. D. J. Kessler, Collision Probability between Orbiting Objects: The Lifetimes of Jupiter's Moons, ICARUS 48, 39-48, 1981.

3.А. И. Назаренко, Построение высотно-широтного распределения объектов в околоземном космическом пространстве, в сб. ИНАС РАН "Проблема загрязнения космоса (космический мусор)",Москва, Космоинформ, 1993.

4. З. Н. Хуторовский и др, Риск столкновений КО на низких высотах, в сб.ИНАС РАН "Столкновения в околоземном пространстве (космический мусор)", Москва, Космоинформ, 1995.

5. Orbital Debris. A Technical Assesment, National Academy Press, Washington, D.C. 1995.

6. Radar Handbook, ed. M. Skolnik, McGraw-Hill, 1970.

APPENDIX

Calculations of approach velocity V and the number of particles Nu(u), passing through unit area (for orbital sector from ascending node to the given value of eccentric anomaly).

Notation:

r - satellite's distance from the center of the Earth;

ρ - unit vector directed from the center of the Earth to orbital position of the satellite;

$\mathbf{n}$, $\mathbf{n}_0$- vectors, normal to the planes of the particle and the platform respectively;

i, i_0 - orbital inclinations of the particle and the platform;

$\mathbf{V}_d$,$\mathbf{V}_p$- velocity vectors of the particle and the platform for the point of approach;

u, u_0 - eccentric anomalies for the point of approach;

ξ - longitude, , χ - latitude;

$z = \sin \chi$.

The orbits of the platform and the particle are considered circular. At the point of orbits' intersection vectors ρ for the particle and the platform coincide.

Approach velocity

$$\mathbf{V} = \mathbf{V}_p - \mathbf{V}_d = V_0 (\mathbf{n}_0 - \mathbf{n}) \times \rho.$$

absolute value of velocity

$$V = V_0 [2(1 - \mathbf{n}\,\mathbf{n}_0)]^{1/2},$$

where V_0 - circular velocity, tangent of approach angle

$$\tan \gamma = (\mathbf{n} \times \mathbf{n}_0)\,\rho / (1 - \mathbf{n}\,\mathbf{n}_0).$$

Representing the vectors in geocentric rectangular coordinates

$$\mathbf{n} = \sin i\,(\sin g\,\mathbf{x} + \cos g\,\mathbf{y}) + \cos i\,\mathbf{z};$$

$\rho = (\cos u \cos g - \cos i \sin u \sin g)\,\mathbf{x} + (\cos u \sin g + \cos i \sin u \cos g)\,\mathbf{y} + + \sin i \sin u\,\mathbf{z} = \cos \chi\,(\cos \xi\,\mathbf{x} + \sin \xi\,\mathbf{y}) + \sin \chi\,\mathbf{z}$, where g - longitude of ascending node, we obtain the relationships

$$(\Pi.1)\quad \mathbf{n}\,\mathbf{n}_0 = [\cos i \cdot \cos i_0 \pm \sqrt{(\sin^2 i - z^2)\cdot(\sin^2 i_0 - z^2)}]/\cos^2 \chi$$

$$(\Pi.2)\quad (\mathbf{n} \times \mathbf{n}_0)\,\rho = [\pm \cos i_0 \sqrt{\sin^2 i - z^2} \pm \cos i \sqrt{\sin^2 i_0 - z^2}]/\cos^2 \chi$$

$$z = \sin \chi = \sin i_0 \sin u_0.$$

The signs of the additives in (П.2) are defined by the signs of cos u, cos u_0, respectively.

The density (per unit area) of particles' flux for short interval dt is equal to $N(r, \chi, \xi)\,\mathbf{V}\,dt = N(r, \chi, \xi)\,\mathbf{V}\,dl/(2V_0)$ where dl - the length of orbital sector, passed by the platform during dt, and the density N is expressed by (2.1). Converting to variable u, we have

$dl = [(d\xi/du)^2 + (dz/du)^2]^{1/2} r\,du = [\sin^2 i_0 - z^2 + \cos^2 i_0 / (1 - z^2)^2]^{1/2} r\,du.$

Two values of velocity correspond to two components of the flux, which will be summed in their absolute values, assuming that the unit area is always directed normally to the flux (assume that the flux passing through the surface of the sphere with unit cross-section is considered). Then the number of particles crossing the unit sphere for orbital sector

(0 , u), is equal to the sum of two additives

$$(\Pi.3)\quad Nu(u) = \frac{N(r,i)}{\pi^2 p} \int_0^u \left[\frac{2(1 - n \cdot n_0)}{\sin^2 i - z^2}\right]^{1/2} \sqrt{\sin^2 i_0 - z^2 + \cos^2 i_0 / (1 - z^2)^2}\,du$$

corresponding to different signs in (П.1).

Numerical integration for (П.3) was performed using trapeze technique with alternating step, decreasing while z approaches sin i, and with approximate integration for the last interval, close to singularity. The case $z \to 1$ for $i_0 = \pi / 2$ gives unlimited increase of the density; however the integrals over the limited area of the field of view or the averaging in inclinations result in finite values. For the sake of simplicity we do not consider this case .

PART 2. THE POSSIBLE STRUCTURE AND VARIANTS OF THE HARDVARE SOLUTIONS

1.INTRODUCTION

The present document is the second part of the report on the problem of creating a MMW radar for monitoring small-dimensional fragments of space debris from board of a space ship [1].

The basis of consideration of the indicating problem is the requirements on creating a radar with minimum power consumption, minimum weight and overall dimensions, high characteristics of reliability that must provide its failure -free operation within a few years [2], as well as some attempts to find the simplest solutions corresponding to the requirements formulated.

Main problems associated with choice of the frequency band, as well as the methods of viewing have been considered in the first part of report [1].

The present study deals with the problems of possible structure of the on-board radar, as well as with the main problems arising when realizing the hardware and software solutions. A brief discussion of possible variants of constructing the hardware is also presented.

2. BLOCK-DIAGRAM OF RADAR

At present Russia [3,4] and USA [5] have accumulated considerable experience on creating radars in K_a-band and bands of higher frequencies. It was found out that, except for the systems of very small power, the transmitting systems are expedient to be developed on the basis of tubes, while the receiving circuits are expedient to be developed with using solid-state devices. Such a construction has just been accepted as a main variant for the radar in question.

A possible block-diagram of the radar and its links to the space ship equipment are presented in Fig. 2.1.

The radar includes an antenna, transmitting-receiving blocks, a block of master oscillator, a block of information processing and control, and a general information bus of "Ethernet" type providing the internal and external links of the radar.

Together with the antenna, the transmitting-receiving blocks provide:

– forming the radiation pattern for transmitting and receiving simultaneously;

– radiation of outgoing pulse and isolation of the receiving circuits for the period of radiation;

– phasing the transmitting and receiving signals;

– reception of the signals reflected from irradiated objects.

The master oscillator block provides excitation of the output devices and synchronization of all the radar components.

It is proposed to use a transmitting-receiving antenna of module type consisting of a few identical blocks. The antenna blocks are arranged in a hexagonal lattice.

The block of information processing and control provides:

– control of the antenna radiation pattern for transmission and reception;

– sampling the signals from the output of the receiving circuits;

– primary detection of the signals within a specified interval of delays when scanning a field of detection;

– detection of the signals during the secondary sounding of the angle direction in which the signal has been detected primarily with the purpose of providing the specified characteristics of detecting the target;

– construction of the detected object trajectories and sending the messages about the trajectory parameters to the ground-based station of tracking space ships.

The transmitting-receiving blocks and block of information processing and control have self-contained power conditioners.

It is assumed that the space ship equipment includes the systems of total time, determination of the space ship orientation, and information reception and transmission providing the on-board radar operation.

The system of the total time provides referencing the radar information to current time and is a source of the reference grids used by the master oscillator block for providing operation of the transmitting-receiving blocks and synchronization of the block of information processing and control.

The system of determination of the space ship orientation provides referencing the radar information to the current position and orientation of the space ship.

The system of transmission and reception of information performs information exchange with the station of tracking the space ship and provides transmission of information about parameters of space debris viewed by the radar.

Radar and space ship connections

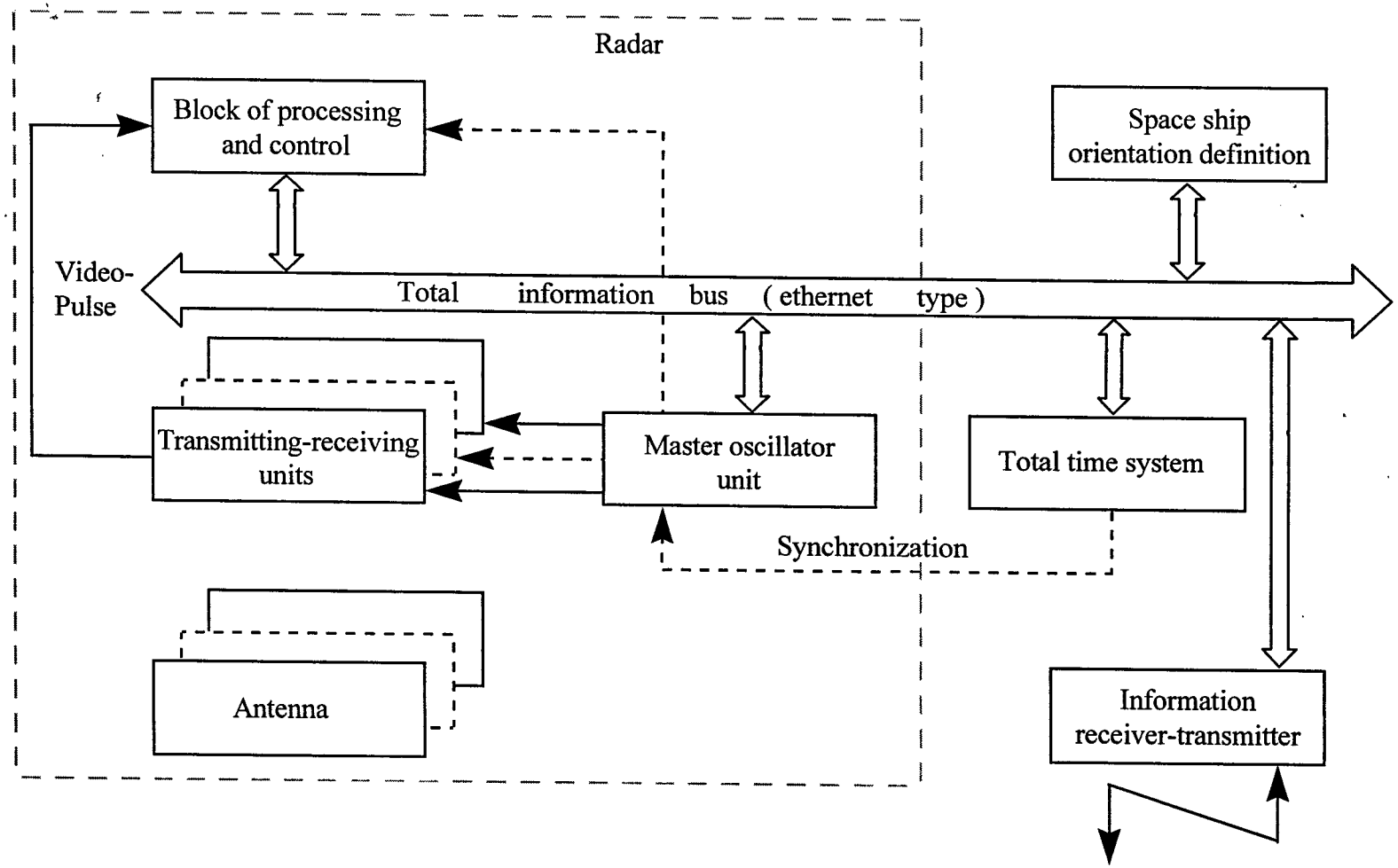

Fig. 2.1.

3. ENERGETICAL AND PRECISION CHARACTERISTICS OF RADAR

Taking into account the requirement of minimal consumed power, we will consider the variant with the plane fence (C1 variant of section 1) as the basic. Transition to the variant with semi-ring fence, which provides more uniform characteristics regarding the area of the field and the accuracy of determination of the target's arrival angle (orbital inclination) is not connected with changes in radar's design and can be fulfilled using the software means. However, the 2db power resource is required.

For providing formation of the barrier sector, the scanning of the radiation pattern is performed in the normal plane to the space-ship velocity, *i.e.* the sector axis is oriented normally to the space-ship trajectory. The number of the radiation patterns in the scan sector is 4-5 (part 1, Fig. 3.1). The pattern width at the level of -3db is ≈5 ' (0.0015 rad), the scan-sector width is ≈14 ' (0.004 rad), the angle between the radiation pattern is ≈3 ' (0.0008 rad). The minimum and maximum detection ranges are 3.6 and 6.2 km, respectively. The minimum time of passing the detection area by an object is $3.5\ 10^{-4}$ s.

For the noise temperature of the receiver 200 K and losses coefficient 0.1 (see 4, 5) the required energy in the pulse is (see 3.3 of part 1) $7.5\ 10^{-3}$ J. Then for the given peak power of the emitter (for the variant, chosen in 4.1 - 1400 Wt for each of the 7 elements of the antenna), the pulse duration is

$$\tau = \frac{E}{P_p} = \frac{7.6 \cdot 10^{-3} j}{1400 \cdot 7} \approx 0.8\ \mu s. \qquad (3.1)$$

For this pulse duration and repetition frequency 25 kHz the pulse period to pulse duration ratio is 50 and the average power per one emitter is - 27 Wt.

If the video signal sampling rate is 2.5 MHz, the number of elements of quantization by range is 44. For radial velocities within the range ±750 m/s and the obtained pulse duration the single –channel filtration in Doppler frequency is possible.

Observation scheme

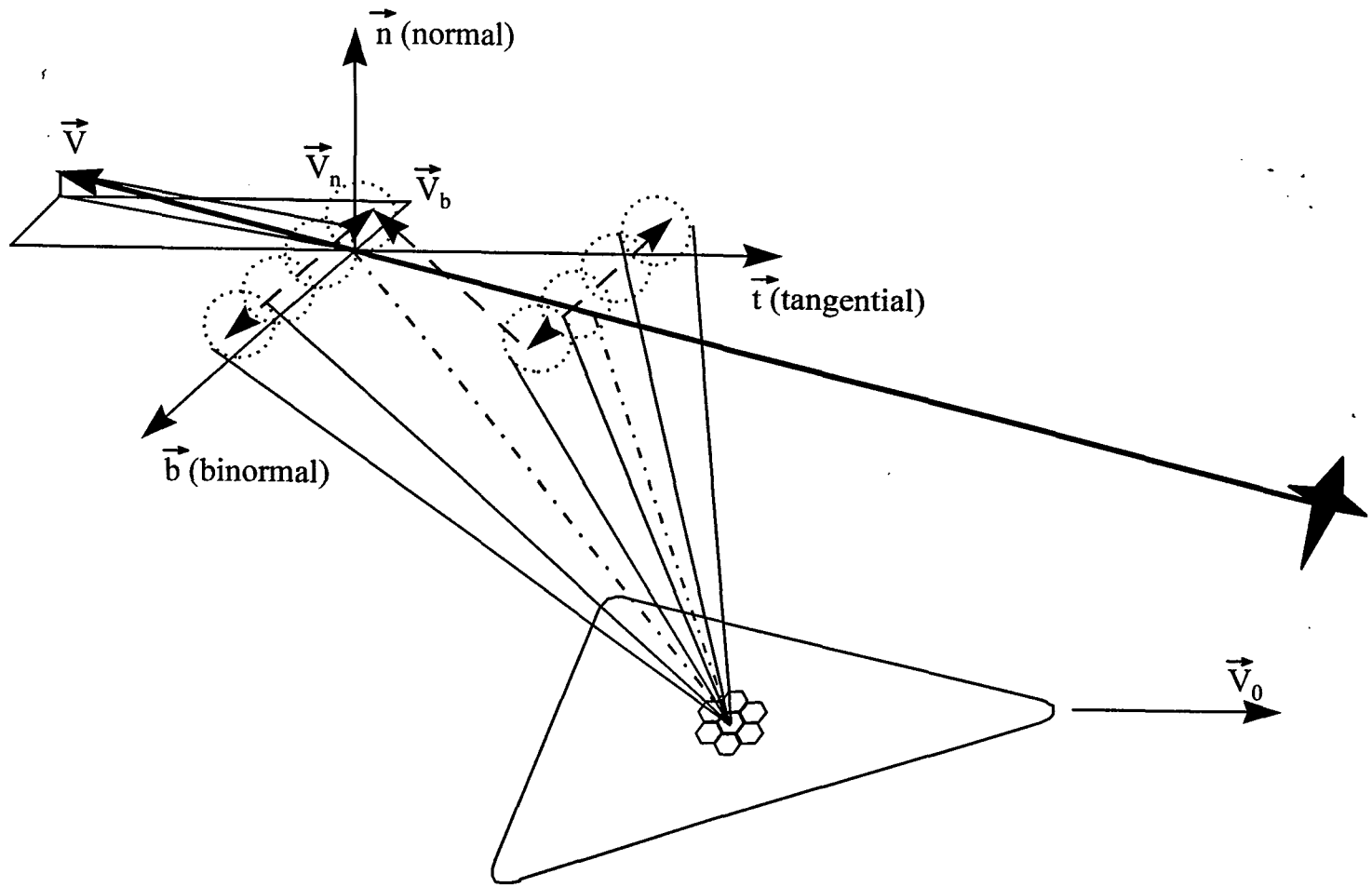

Fig. 3.1.

If the intensity of appearance of the space debris fragments is one object a day [2], the intensity of wrong detection of the objects is expedient to be chosen of the order of 0.05 a day.

To achieve the required value of the wrong detection intensity, it is supposed to use a procedure of two-stage detection. An object is considered as a detected one in case of detection of the object signal on the first stage during the primary sounding of the angular direction in the area of detection by a single sounding pulse with the subsequent confirmation of detecting the object signal on the second stage during sounding by a pair of pulses in the same angular direction as that determined on the first stage.

The probability of exceeding the detection threshold by noise on the first and second stages is 0.00005 and 0.0001, respectively.

The probability of the object detection for the indicated signal-to-noise ratio is no less than 0.95 with taking into account of no less than two irradiations of the object within the time of its going through the barrier sector. For the signal-to-noise ratio indicated above:

– the root-mean-square error of measurement of the object effective scattering surface does not exceed 1-to-2 dB;

– the total root-mean-square error of the angle estimation by the measurement of the signal amplitudes in the neighbor angular directions does not exceed 0.6 angular minutes;

– the total root-mean-square of the range estimation does not exceed 9 m.

To determine the velocity vector components (tangential, normal and binormal to the space ship trajectory) of the object moving, the barrier sector after detection is displayed in the direction opposite to the space ship velocity vector by 10 angular minutes with delay of no more than 0.00007 s.

The tangential component of the object velocity vector is in the limits of 0-to-15 km/s.

The normal component of the object velocity vector is in the limits of 0.75-to-0.75 km/s.

In the displaced sector position, the viewing of the sector for detection of an object moving through it is being performed within 0.020 s. After expiration of the indicated time, the sector returns to its previous position.

At the signal-to-noise ratio of 15 dB, that procedure allows providing the measurement of the tangential and binormal components of object movement velocity with the root-mean-square error not exceeding 250 m/s. The root-mean-square error of the object velocity normal component does not exceed 1000 m/s at the tangential component of the object velocity equal to 7500 m/s.

With high probability, the procedures of the object trajectory detection indicated above allow excluding the object trajectory detection by the side lobes of the radiation pattern because their position and level sharply change when scanning.

The use of an active phased array allows forming other configurations of beams when viewing [1]. The final choice of an expedient beam configuration must be made at the stage of the radar development.

4. TRANSMITTING-RECEIVING BLOCK

4.1. Main characteristics

The transmitting-receiving block must provide amplification of sounding signals, reception and amplification of echo signals, and protection of the receiving circuits from the penetrating signal. The synchronization of the block is performed from the system of the total time. The block comprises the transmitting and receiving modules and provides the following main parameters:

– carrier frequency, GHz 95;
– output peak power, kW 1.4;
– pulse duration, μs 0.8,
– pulse recurrence rate, kHz 25;
– gain, dB 40;
– noise figure, dB 2.5;
– dynamic range of input signals, dB 60;
– time of parameters recovering after penetrating power affecting, μs 0.2.

The basic element of the transmitting module that mainly determines the scheme of construction of the module is the amplifying microwave device. The module VZB2783 from Company VARIAN (Fig. 4.1) complies with the requirements indicated above. It has the following parameters:

– central frequency, GHz 95;
– frequency band of amlplification, MHz 1000
– output peak power, kW 1.4;
– output average power, W 50
– gain, dB 45;
– pulse duration, μs 2;
– pulse period-to-pulse duration ratio 25;
– voltage of direct current power supply, V 270;
– mass, kg 3.2;
– overall dimensions, mm 80×100×244;
– cooling air

A device with close characteristics in the band of 95 GHz has been developed in Russia as well.

For providing the requirement on the noise figure, the low-noise amplifier (LNA) of the receiving module can be performed by the technology of monolithic integrated circuits on the basis of pseudomorphic InP HEMP [6]. The monolithic one-cascaded LNA performed by the indicated technology provides the noise figure of 1.3 dB for gain of 23 dB in the mode of small signal.

The device of the LNA protection from penetrating power of the transmitters can be performed either in the form of a semiconductor limiter or in the form of a *pin*-diode switch.

It is expedient to consider an implementation of the transmitting module in a solid-state modification. At present, the following power levels have been achieved in the solid-state devices at frequency of 95 GHz:

– 10-to-50 mW in the transistor amplifiers;
– 20-to-40 mW in the frequency multipliers.

Providing the necessary peak power of 1.4 kW requires using 30000-to-150000 transistor amplifiers instead of one klystron. In this case there must be used an active antenna system in which each of the microwave signal sources has its own radiator, and the power addition is performed in air. If the gain of one transistor amplifier is 20 dB, it is necessary to provide total peak power of about 14 W at the amplifier inputs in one transmitting-receiving block. The excitation of 30000-to-150000 transistor amplifiers can be performed by the optical method with the signal loss of approximately 10 dB. All the other methods of excitation will give much more loss. Thus, excitation of the indicated number of the transistor amplifiers will require a microwave signal source with peak power of 140 W. Such power can be provided only a vacuum device like a klystron of a traveling-wave tube.

Communications & Power Industries
45 River Drive / Georgetown / Ontario / Canada / L7G 2J4

MILLIMETER WAVE POWER MODULE

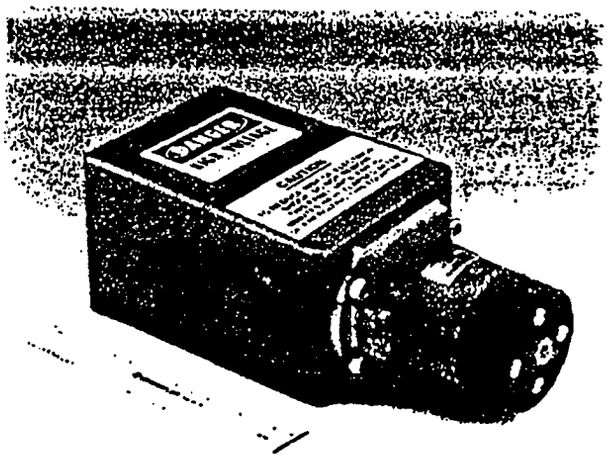

The VZB2783 series of Miniaturized Millimeter Wave Power Modules are ideal for airborne and mobile applications. These modules are a compact, high power alternative where solid state sources cannot provide RF power at high efficiency. Efficiencies over 10 times that of solid state can be achieved with expected life times of 5 - 10 years. The small footprint power module is under development. Please call Varian for details.

PERFORMANCE

ELECTRICAL

• FREQUENCY	93 to 96 GHz
• PEAK OUTPUT POWER	1.4 kW
• AVERAGE POWER	50 WATTS
• BANDWIDTH	1.0 GHz
• GAIN	45 dB
• PRF	100 kHz
• PULSE WIDTH	2 μS
• DUTY	.04
• PRIME POWER	270 V DC

MECHANICAL

• WEIGHT	7 lbs
• DIMENSIONS	3 1/8" x 3 7/8" x 9 1/2"
• WAVEGUIDE	WR 10 (.050 X .100 ins.)
• FLANGE	UG-387/U modified
• COOLING	FORCED AIR

Communications & Power Industries
45 River Drive / Georgetown / Ontario / Canada / L7G 2J4

Telephone: (905) 877-0161
Fax: (905) 877-5327

varian

ISO 9001 REGISTERED

Fig. 4.1.

The efficiency of the transistor amplifiers at frequency of 95 GHz is approximately equal to 5%. The consumed power of the transmitting module will be two times greater in comparison with the case of using a klystron. Correspondingly, the heat release of the equipment will be twice as much. The optical method of excitation of an active antenna system with a very dense arrangement of the transistors in the antenna aperture allows organization neither air nor liquid systems of cooling.

For the cost of one transistor amplifier of \$50-to-\$100, the cost of only transistors in the active system of one transmitting-receiving block will amount to \$1500000-to-\$15000000, while the cost of an amplifying module on the basis of a klystron will be \$100000-to-\$200000, *i.e.* by two orders below.

The transmitting module can be built also on the basis of frequency multipliers. The available frequency doublers have maximum conversion efficiency of the order of 40%. They just can be used as the microwave signal sources in the active antenna system. In this case, the excitation is performed at the two times less frequency of 42.5 GHz. The problems arising in creation of an antenna system with using the multipliers are similar to those described above for the transistor amplifiers.

Thus, the attempt to develop a radar transmitter on the basis of the solid-state sources will result in:

– the necessity of using the vacuum devices of approximately the same class as in the main variant with all the resulting negative consequences associated with the use of the vacuum devices;

– increase of the power consumption and heat release.

This case also leads to the very difficult problems of removing the heat from the equipment, that is associated with high density of the element arrangement, and to increasing the equipment cost by 15-to-150 times.

In this connection, the development of the radar on the basis of the solid-state sources seems currently to be inexpedient.

The block of the master oscillator provides excitation of the transmitting modules and the necessary synchronization of the radar equipment.

4.2. Scheme of construction

A simplified block-diagram of the microwave part of the radar is presented in Fig. 4.2.

The transmitting module is a pulse amplifier of microwave signals at the carrier frequency of 95 GHz. A klystron in the module is used as a microwave amplifier. The peak power at the output corresponds to 1.4 kW with providing gain of 45 dB.

The receiving module performs amplification of echo signals at the carrier frequency of 95 GHz, conversion of the signals to the intermediate frequency, and transmission of them to the circuit of forming the sum signal.

Control of the phase of the signals when radiating and receiving is performed with using phase shifters installed at the receiving module output and at the klystron input in the transmitting module. Control of the phase shifters is performed by the codes coming from the block of information processing and control.

Each module is provided with power conditioners built by the scheme of conversion of a direct voltage into an alternating one with frequency of 100-to-200 kHz and 90% efficiency.

The receiving module provides one-channel processing the echo signals within the whole range of the Doppler frequencies.

The noise temperature of the receiving module reduced to its input is calculated by formula

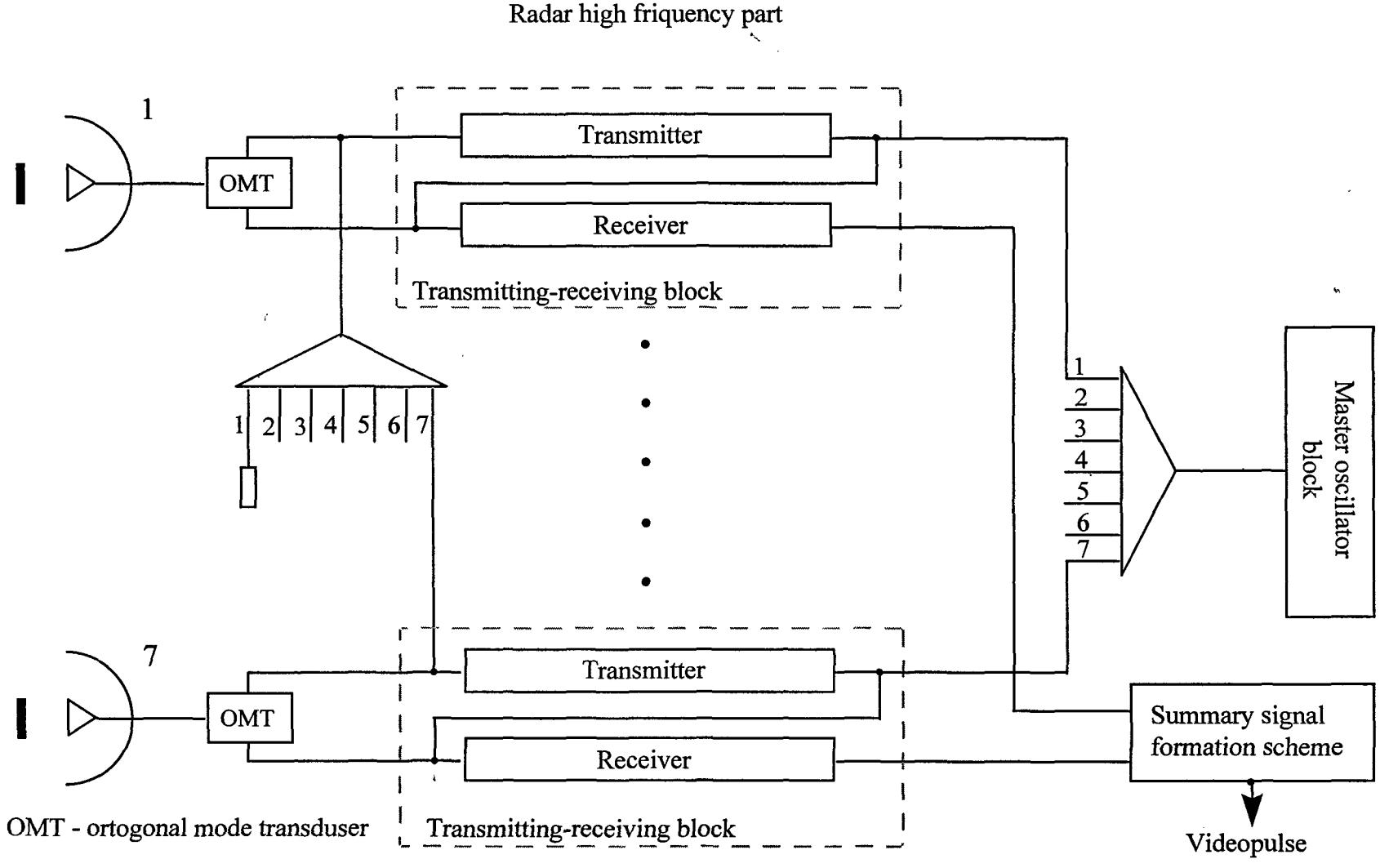
Radar high friquency part
1
OMT
Transmitter
Receiver
Transmitting-receiving block
1 2 3 4 5 6 7
1
2
3
4
5
6
7
Master oscillator block
7
OMT
Transmitter
Receiver
Summary signal formation scheme
OMT - ortogonal mode transduser
Transmitting-receiving block
Videopulse

Fig. 4.2.

$$T = T_{prot} + \eta_{prot}[T_{LNA} + (T_{MX} + \eta_{MX} T_{IFA})/G_{LNA}], \quad (4.1)$$

where T_{prot} = 33°K is the protection device noise temperature determined by the device loss;

η_{prot} = 0.5 dB is loss in the protection device;

T_{LNA} = 95 °K is the noise temperature of the LNA;

G_{LNA} = 30 dB is the LNA gain;

T_{MX} = 870 °K is the mixer noise temperature determined by the mixer loss;

η_{MX} = 8 dB is loss in the mixer;

T_{IFA} = 10000 °K is noise temperature of the intermediate frequency amplifier.

The calculated noise temperature relative to the receiving module input amounts to about 210 °K.

The block comprises elements for automatic maintaining the stability of phase and transmission coefficient of seven receiving modules.

For maintaining the stability of the transmitting and receiving channels, the radar design must satisfy the following conditions. All the seven transmitting-receiving blocks must have the temperature spread of no more than $\pm 10^0$C. For this reason, they must be shielded by a light-reflecting material with small heat coductivity. The space ship design must be provided with special panels for heat removal from the transmitting-receiving blocks.

The possible power consumption of the transmitting module is evaluated for the following parameters: the output peak power is 1.4 kW, the pulse duration is 0.6 μs, the pulse recurrence rate is 30 kHz, and the klystron efficiency is 10%. The average power consumed by the klystron will amount to about 280 W.

The value of the modulator efficiency with the power conditioner taken for the calculation of the transmitting module power consumption is 90%. The power consumption of the transmitting module will amount to about 310 W. The receiving module power consumption will be 15 W. Thus, the power consumption of the transmitting-receiving block will amount to approximately 325 W.

The longevity of the block will approximately amount to 50000-to-80000 hours. The equipment longevity is mainly determined by the klystron longevity. High longevity of the klystron is assumed to be achieved at the expense of its using with loading for 50% by average power.

The mass of the transmitting-receiving block will approximately amount to 8 kg.

5. ANTENNA

5.1. Antenna characteristics and scheme of construction

The Phased Array Antenna consists of seven Large Aperture Radiators (LAR), that are arranged on a load-carrying structure. The centers of all the LAR apertures lie in one plane in nodes of a hexagonal lattice (Fig. 5.1). Every LAR is performed as a Cassegrain antenna and contains a main reflector, a subreflector with thrusts, a primary feed and a waveguide feeder. The main reflector is a symmetrical paraboloid. Edges of the reflector are cut so that its projection onto the aperture plane is a regular hexagon with a side of 380 mm. In this case the aperture of the array as a whole is inside a circle of 2 m in diameter. The feed of each LAR is a dual-mode Potter horn. The subreflector is hyperbolic and axis-symmetrical.

General View of Antenna

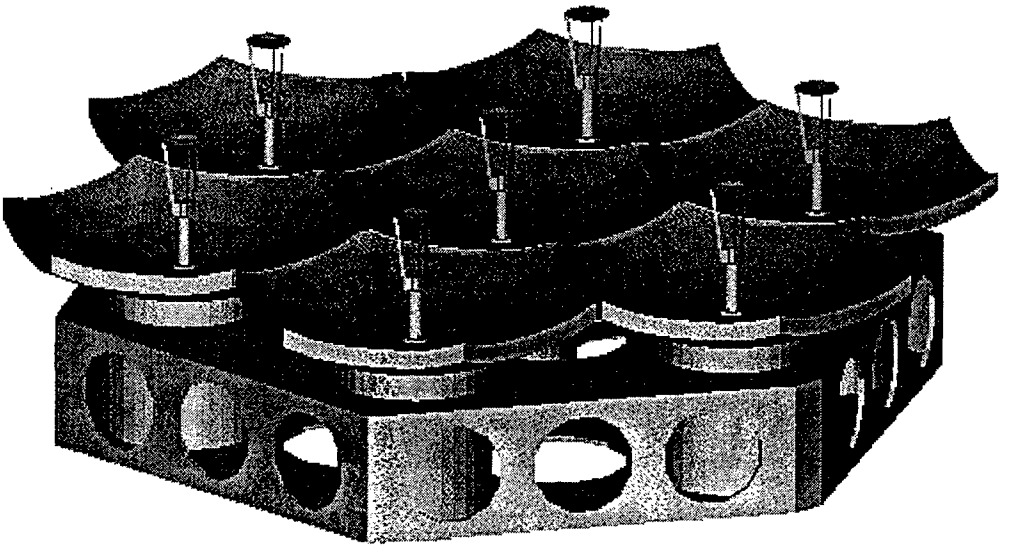

Fig. 5.1.

Coherent signals are given to the LAR's inputs. For scanning by the main beam of the pattern it is necessary to produce linear phase distributions between LAR's in planes of phasing, i.e. to give a signal with a corresponding phase to each LAR input. An angle sector of electric scanning is limited by the beam width of a separate LAR and it is assumed being equal to ±7.5 angle minutes in any plane.

In Fig. 5.2 the calculated pattern of the array antenna is presented when the beam is axis-directed, i.e. when all LAR's are excited in phase. Two the main sections of the pattern in vertical and horizontal planes are shown at the top of Fig. 5.2; the map of the pattern levels in dB is given at the foot, where the structure of side lobes is seen distinctly. A particular feature of the given array antenna is a small number of radiators and very large step of array: it is 328 mm in vertical plane (103 of wavelength) and 564 mm in horizontal plane (177 of wavelength). The consequence of the big step of array is a small angle distance between interference maximums, that is well seen at the foot of Fig. 5.2. In accordance with the calculation, the half power beamwidth level is equal to 6.2 angular minutes and the gain equals to 63.4 dBi with taking into account the loss in the LAR feed's waveguide. At that an efficiency of a separate LAR is equal to 0.72.

During scanning a main lobe of the pattern deflects from the axis direction. The patterns of the array antenna for the cases when the beam is maximally deflected by 7.5 angular minutes in horizontal and vertical planes are presented in Fig.5.3 and 5.4 correspondingly. The patterns are normalized to the maximum of the non-deflected beam. Because of the interference maximums are very close to the axis direction they move during scanning and come to a region of the main lobe of a LAR pattern. As a result their contribution to the antenna array pattern increases very much even when scan angles are small. Thus, the side lobe level increases up to – 2 dB with respect to the main lobe maximum in the case of the maximum deflection, as it may be seen in Fig. 5.3. A gain of the antenna array main lobe decreases by approximately 2 dB at the edge of the scan angle sector.

Two ways are possible to struggle against the high side lobes. The first way is obvious – it is to decrease the LAR dimension till the value when not 7 but 19 elements of hexagon lattice are inscribed in a circle of 2 meters in diameter. In this case array spacing should be reduced by about 1.7 times that leads to the same increase of the angle distance between interference lobes. The phenomena of their increasing during scanning appears in less extent and a side lobe level should not exceed –10 dB. Another way is to remove the interference lobes by means of algorithm, during processing an information. The first way is possible and has not any principal limitation, but it assumes a more complicated antenna design. So, the second way is more preferable and it is considered as the main one.

5.2. Description of design

The design of the antenna includes seven identical LAR and a supported structure (rigid framework), on which they are attached rigidly. Because of the antenna should form a very narrow beam there are very hard demands on an accuracy of maintaining and mutual adjusting of all LARs and also on a mechanical stability of the design during operating. One of the main factors affecting on antenna is the sun radiation, that cans cause an irregular heating and deformation of design. Heat insulation materials, being traditionally used for covering equipment operating in free space, are not suitable for an aperture part of antenna. Besides, the antenna mass should be minimized. So, it is necessary to use materials with high specific rigidity and low thermal expansion factor.

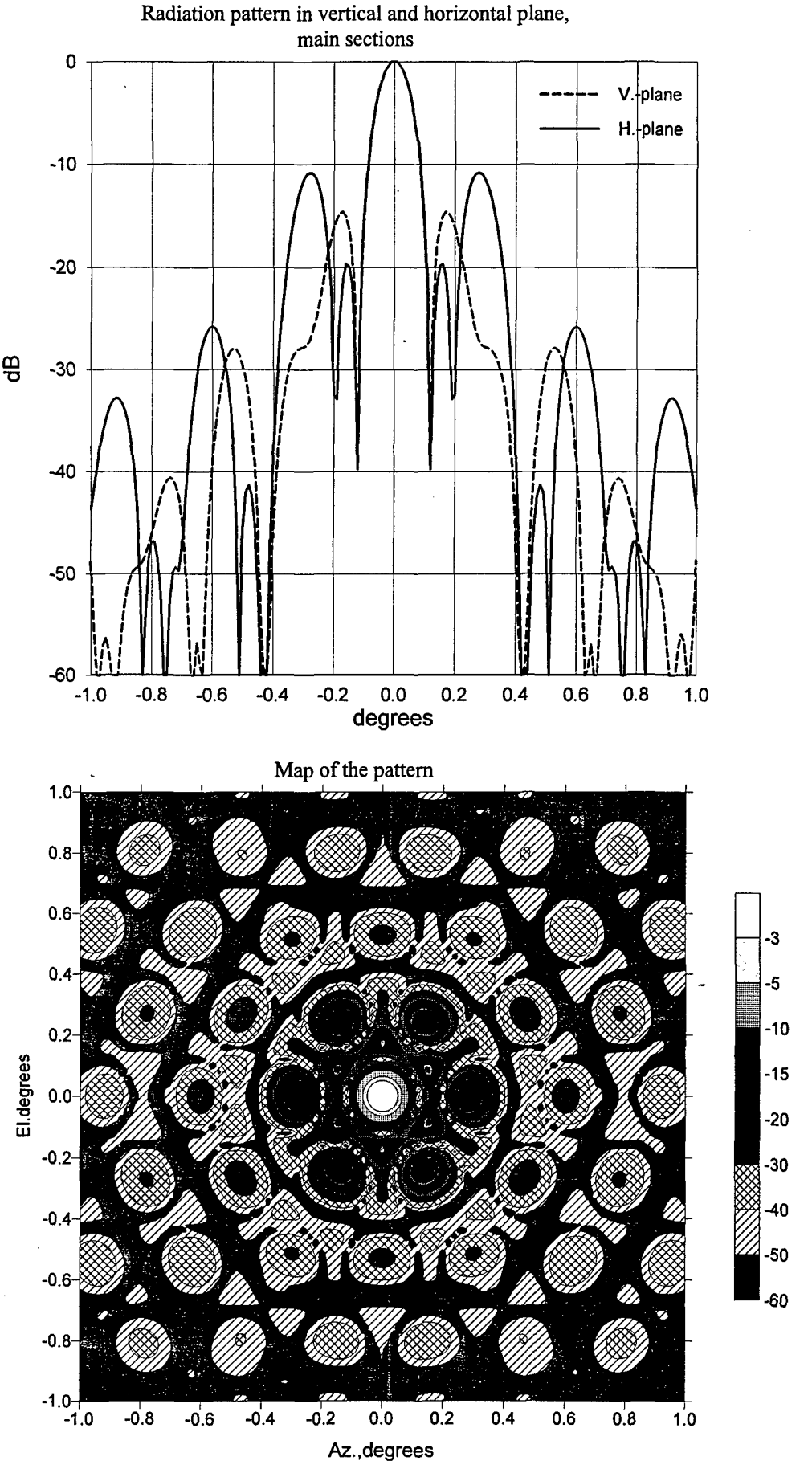
Radiation pattern in vertical and horizontal plane,
main sections
V.-plane
H.-plane
dB
0
-10
-20
-30
-40
-50
-60
-1.0
-0.8
-0.6
-0.4
-0.2
0.0
0.2
0.4
0.6
0.8
1.0
degrees
Map of the pattern
El.degrees
Az.,degrees
-3
-5
-10
-15
-20
-30
-40
-50
-60

Fig. 5.2

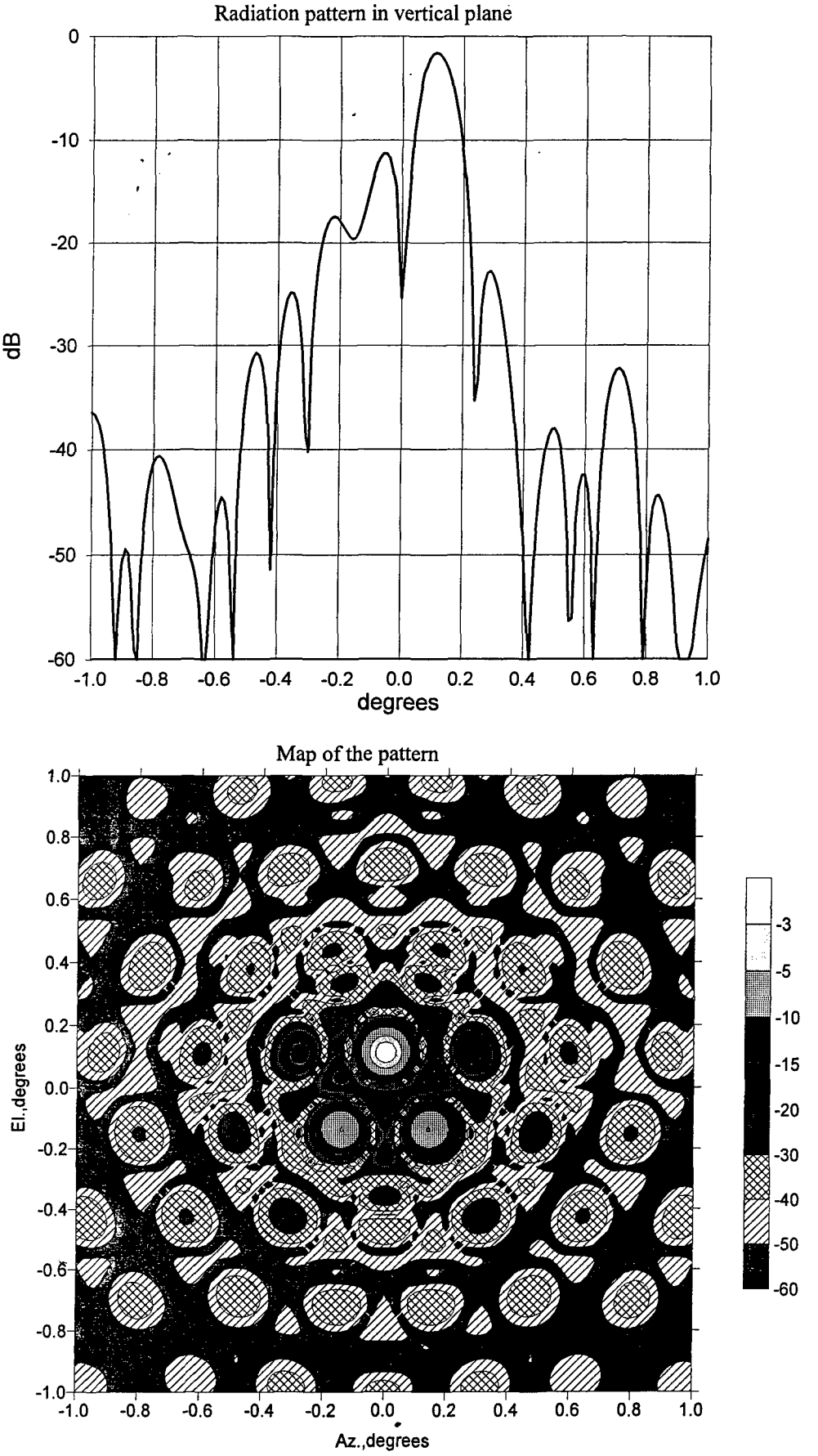
Radiation pattern in vertical plane
dB
0
-10
-20
-30
-40
-50
-60
-1.0 -0.8 -0.6 -0.4 -0.2 0.0 0.2 0.4 0.6 0.8 1.0
degrees
Map of the pattern
El.,degrees
1.0
0.8
0.6
0.4
0.2
0.0
-0.2
-0.4
-0.6
-0.8
-1.0
-1.0 -0.8 -0.6 -0.4 -0.2 0.0 0.2 0.4 0.6 0.8 1.0
Az.,degrees
-3
-5
-10
-15
-20
-30
-40
-50
-60

Fig. 5.3

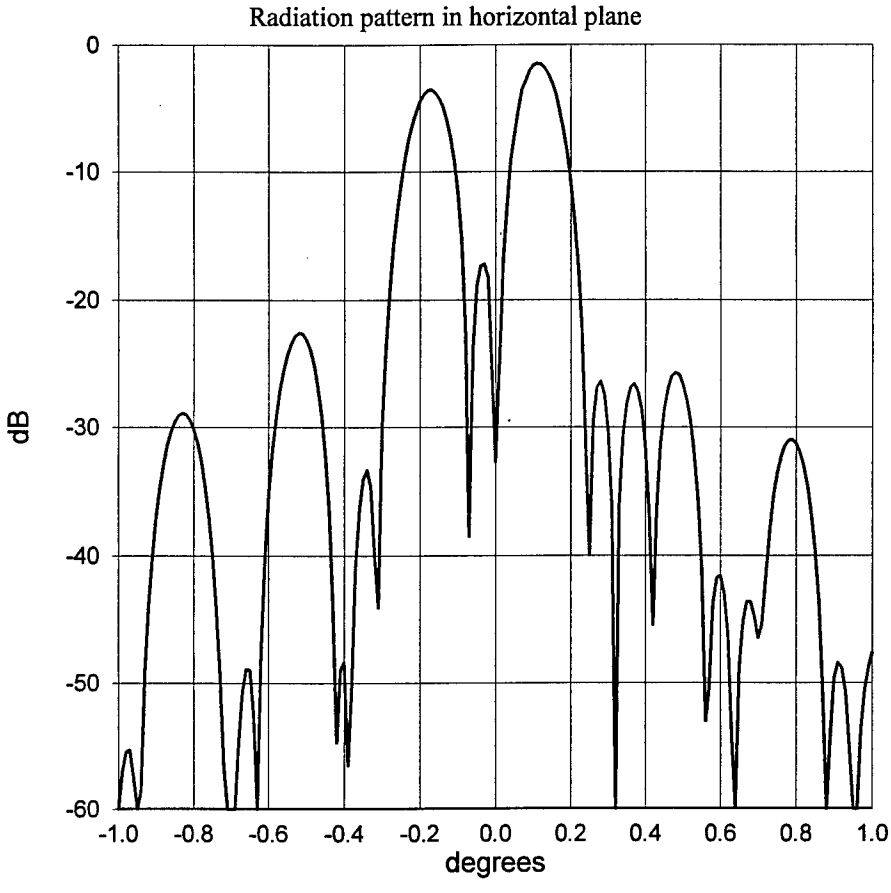
Radiation pattern in horizontal plane
dB
0
-10
-20
-30
-40
-50
-60
-1.0
-0.8
-0.6
-0.4
-0.2
0.0
0.2
0.4
0.6
0.8
1.0
degrees

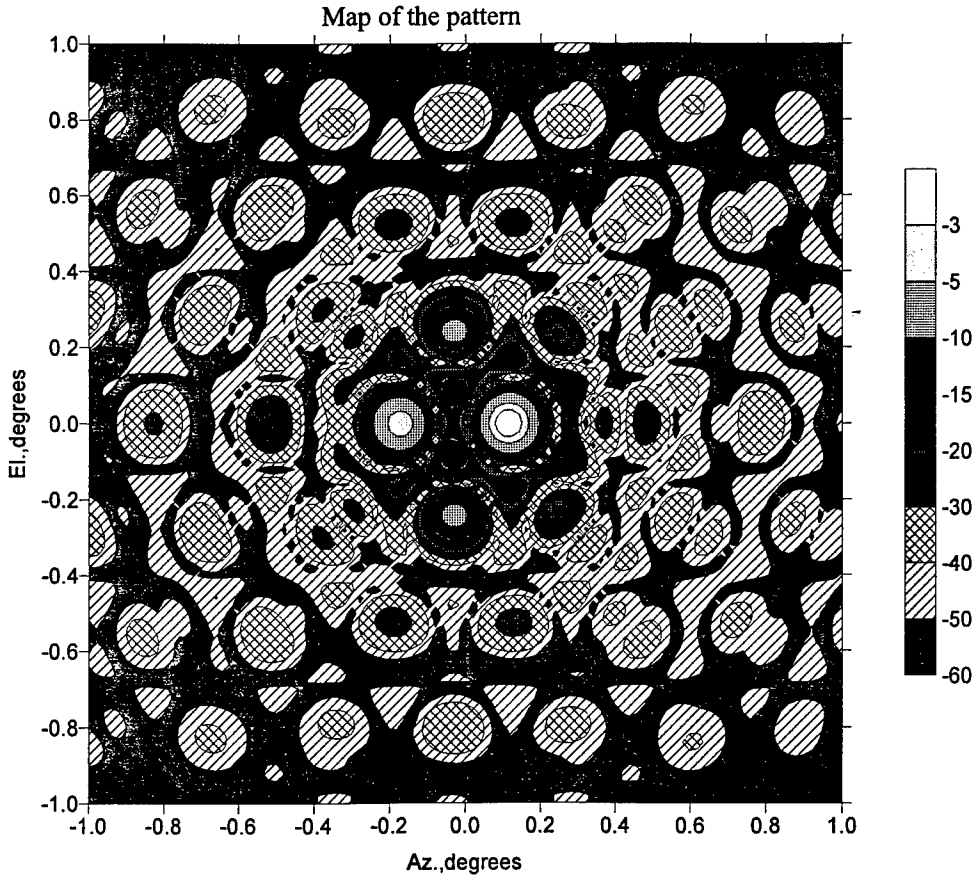
Map of the pattern
El.,degrees
Az.,degrees
1.0
0.8
0.6
0.4
0.2
0.0
-0.2
-0.4
-0.6
-0.8
-1.0
-3
-5
-10
-15
-20
-30
-40
-50
-60

Fig. 5.4

The experience of creating such antennas for spacecrafts in Russia says about necessity of using composite materials on a basis of carbon fibers (carbon-plastics). Epoxy resin of cool or hot hardening is used as filler. The technology of producing high-precise reflectors from carbon-plastics is developed and is used widely. The value of standard deviation of a reflector surface from ideal form can be made no more than 0.1 mm. The good rigidity properties of this material with small mass permit to use it also for making the antenna supported structure. Elements of the frame, being made of carbon-plastics, are placed to an assembly jig and are jointed together by glue. The subreflector and the feed for LAR are produced of metal. The technology of galvanic building up is used for waveguide manufacturing.

As an example, the construction of Ku-band multi-beam antenna, produced in JSC"Radiophizika" (Moscow), may be considered. It has 3- meters reflector (Fig. 5.5). The antenna is provided by the opening mechanism, that begins its operating in orbit by a command. The reflector and the support structure are made of carbon-plastics. The support structure and the reflecting envelope of the reflector are isolated mechanically one of another. Together with the choice of material this permits practically to exclude heat deformations in orbit. A weight of the reflector is 40 kg, a total weight of the antenna is 126 kg.

Carbon-plastics reflects electromagnetic field sufficiently good and, in principal, it may be used as reflector without additional metallization in Ku-band. Nevertheless, when operating at frequency 94 GHz the influence of a carbon fibers structure may be arise in form of not desirable depolarization and scattering of field. If these effects are strong in practice, the working surface of reflectors would be metallized by plasma spraying process in vacuum. A smoothness of a surface is provided by filler.

A mass of the seven LARs is estimated as 12–20 kg, a mass of the support structure is about 18–20 kg. Thus, a total mass of the antenna is approximately 30–40 kg. No active elements are in the antenna, so a consuming of energy is absent.

6. BLOCK OF INFORMATION PROCECCING AND CONTROL

6.1. Scheme of construction

The conditions of operating as well as the requirements for the weight and overal dimensions characteristics define the necessity of using microprocessors when creating the block of information processing and control.

A possible block diagram of the block in question is presented in Fig. 6.1.

The block is realized on the basis of the system bus VMEbus64 and includes a signal processor module DSP and a central processor module V5A. The processor modules are arranged in a VME-crate where a room is provided for arrangement of a board with a hard disk drive (HDD) and a floppy disk drive (FD) to be used for the period of debugging and adjusting the block. An output of the ETHERNET channel is provided from the module V5A to which a computer is connected for software debugging in real time. The VME-crate of a hermetic implementation includes a power conditioner.

The modules DSP and V5A are linked to each other over the system bus VME. The module V5A has an output to the common information bus of the space ship through a PCI add-in (a PMC board), and provides information exchange with the space ship equipment. The control of the mode of digitizing the video pulses in the current interval of the sounding pulse is performed by means of transmitting the corresponding information at the end of the previous interval of sounding. The pulses of 30 kHz frequency are sent to the modules DSP and V5A for synchronization of their operation. The pulses with frequency of digitizing the video pulses of 2.5 MHz are sent to the module DSP.

Carbon – plastic Ku–band Antenna
for Communication Satellite

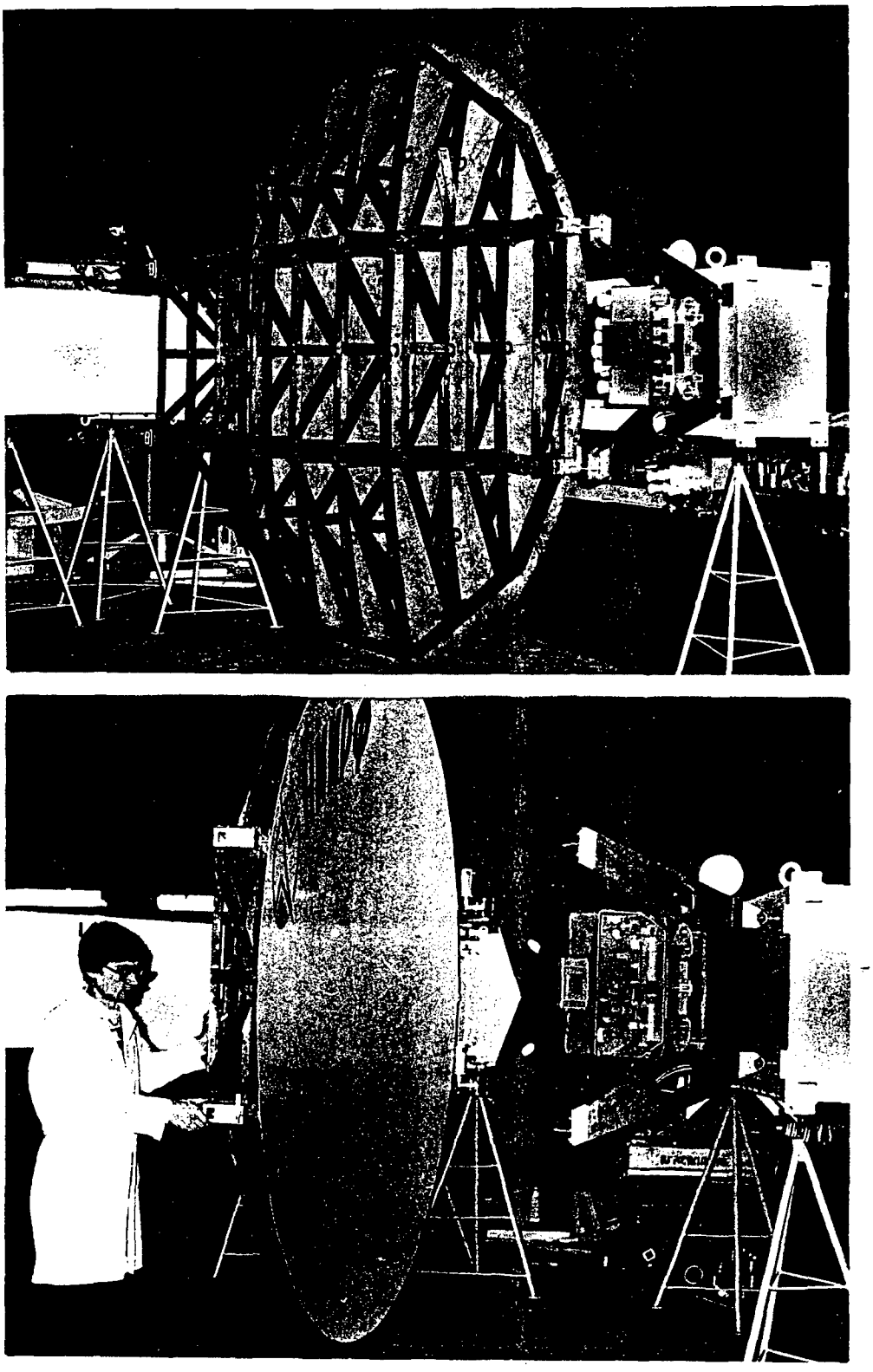

Fig. 5.5.

Block processing and control

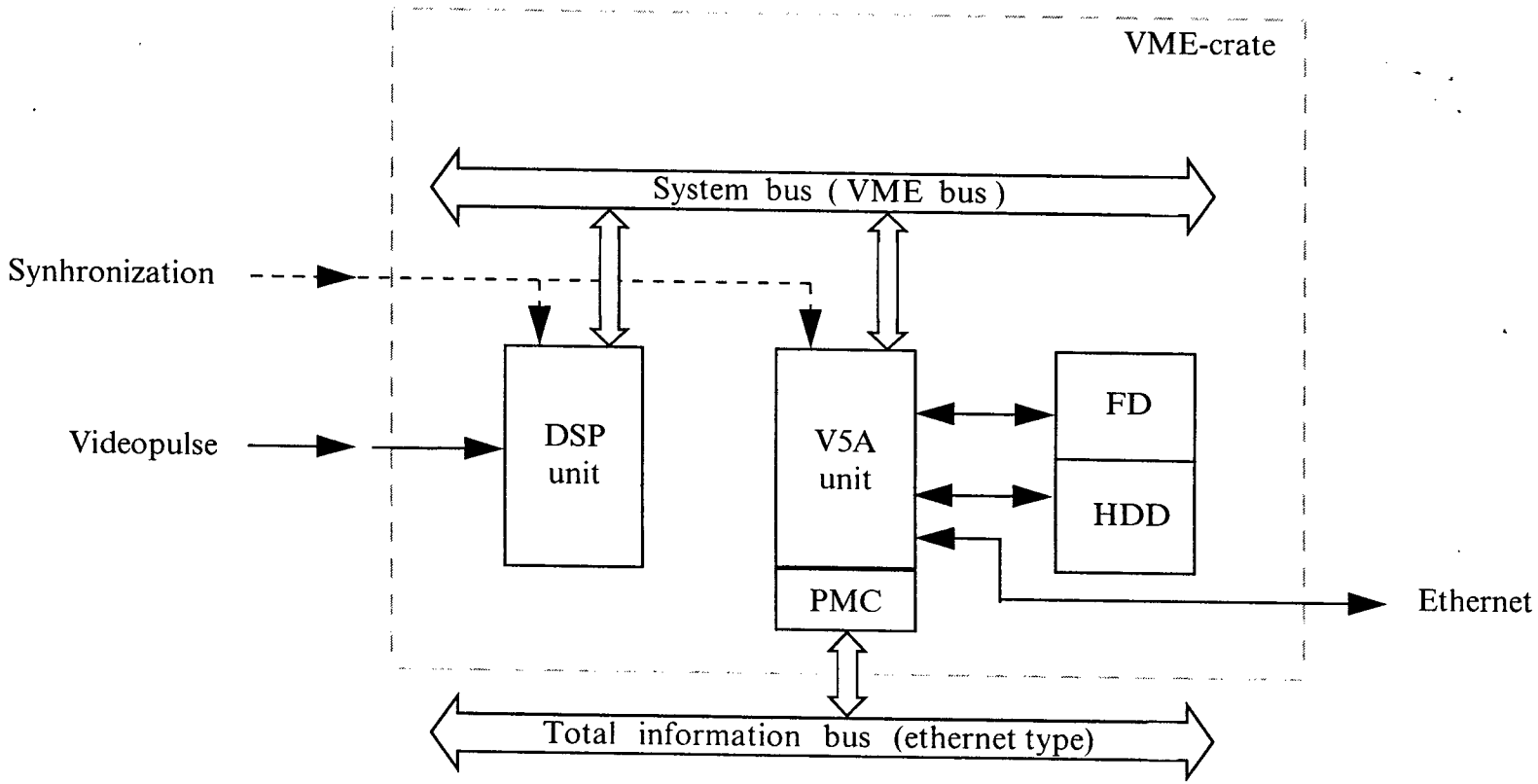

Fig. 6.1.

The overall dimensions of the block of information exchange and control are determined by the VME crate dimensions, and the weight and power consumption of the block are negligibly small in comparison with the corresponding parameters of the radar as a whole.

6.2. Signal processor module

A possible block diagram of the signal processor module (unit) DSP is presented in Fig. 6.2.

The module DSP is performed on the basis of a TIM module for entering and digital processing the signals DST40A50/AD8x40M (DST40A40/AD8x40M), and a multiprocessor module for digital signal processing.

The TIM module consists of a 8-bit analog-to-digit converter with sampling frequency of 2.5-to-40 MHz, a 32-bit digital processor TMS 320C40 with maximum performance of 50 (40) MFlops, a buffer FIFO between the analog-to-digit converter and processor, and a 512 Kbyte cache for storing programs and data.

The multiprocessor module of digital signal processing consists of:

– 3 signal processors TMS320C40GFL50 connected by the scheme "each to each" by means of links;

– 4 blocks of static memory of 1 Mbyte capacity each:

– 3 block of local memory (LM) (one block for each processor);

– 1 block of shared memory accessed by writing and reading both from the side of the zeroth processor and from the bus VME;

– 2 blocks of dynamical memory (DM), by 16 Mbytes each, connected to the processors with numbers 1 and 2;

– 1 Mbyte of flash memory used for storing the programs;

– a local control device;

– a universal controller of bus VME VICO68A;

– two serial ports RS-232.

The module DSP has the following technical characteristics:

– total performance up to 150 MFlops;

– total volume of static memory of 5 Mbytes;

– total volume of dynamical memory up to 32 Mbytes;

– flash memory of 1 Mbyte;

– consumed power of no more than 50 W;

– overall dimensions of 160×233 mm, is performed according to the standard VMEbus IEEE 1014-87;

– mass of no more than 0.7 kg.

6.3. Central processor module

The central processor module (unit) V5A is a single board VME computer compatible with a PC/AT.

The block diagram of the module V5A is shown in Fig. 6.3. The module is built on the basis of a PENTIUM processor with a free system bus VMEbus64 allowing to create multiprocessor computer systems. The module V5A provides all the interfaces used in personal computers IBM PC/AT.

DSP unit block diagram

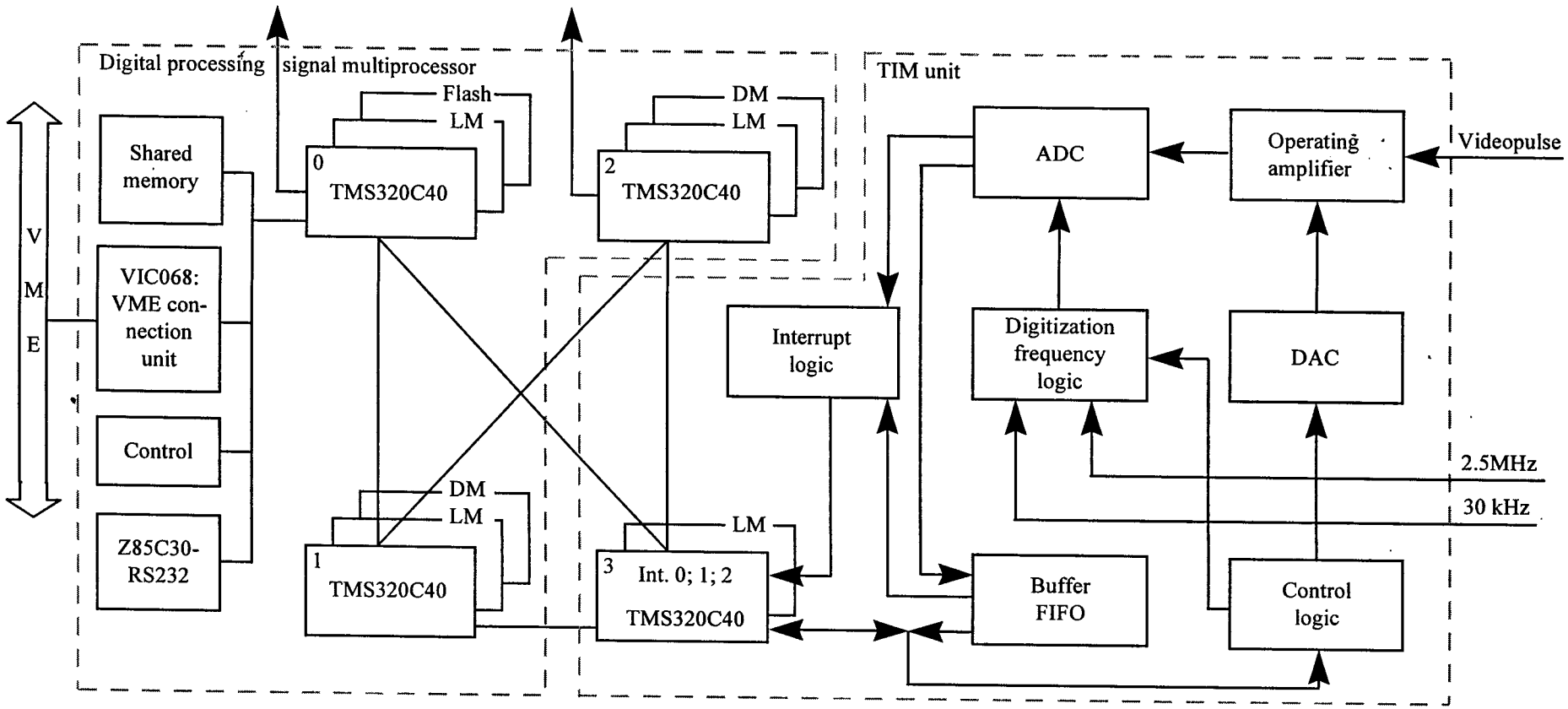

ADC - analog - digital conversion;
DAC - digital- analog conversion;
LM - local memory;

DM - dinamic memory;
Flash - Flash memory.

Fig. 6.2.

V5A unit structure scheme

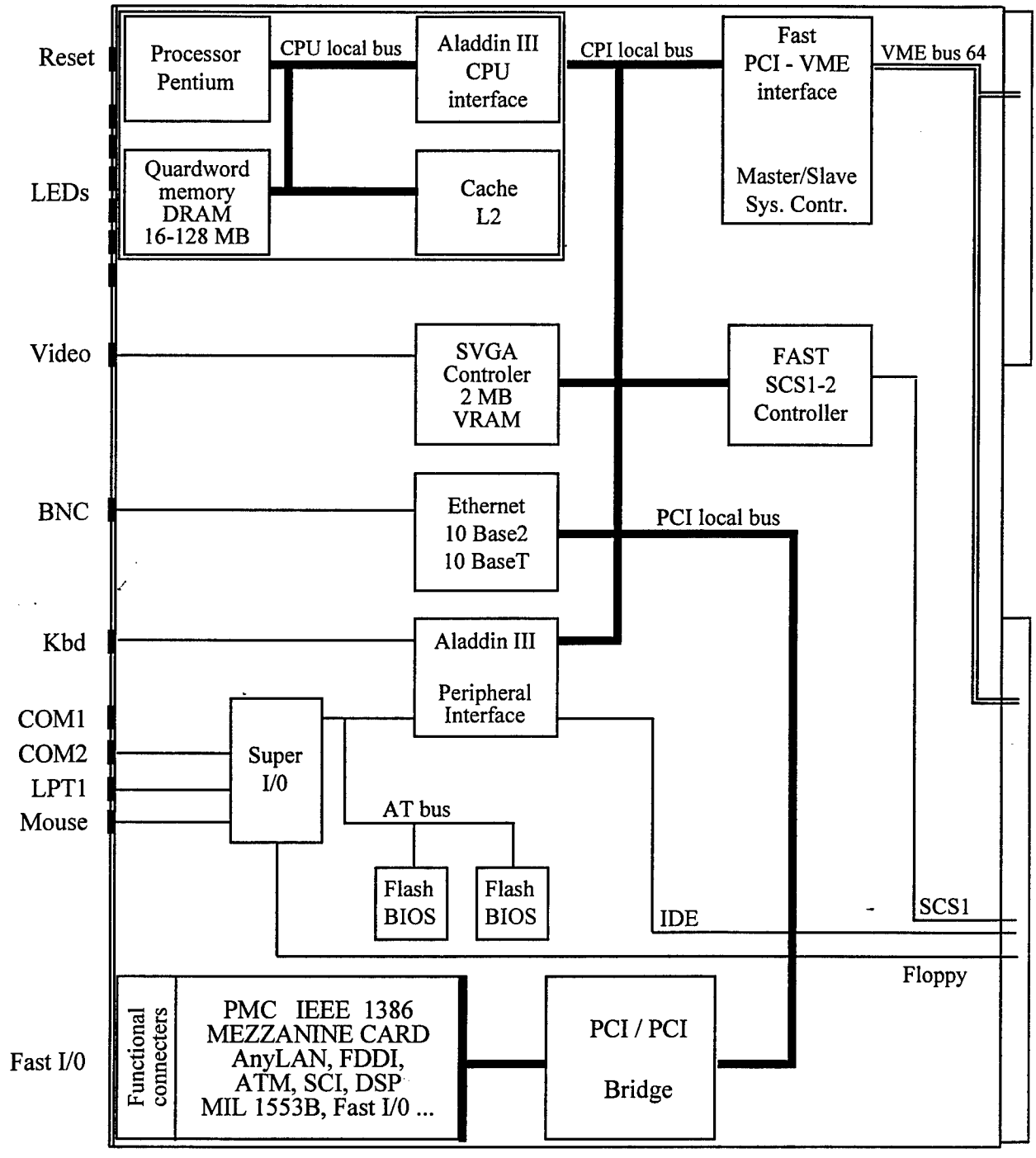

I/0 - input/output
Kbd - keyboard
CPU - central processor unit
LEDs - light-limitting diodes

Fig.6.3.

The module V5A comprises an implemented PCI add-in corresponding to the International standard of on-board add-ins PCM IEEE 1386.1. That allows enhancing the operating capabilities of the module by a simple installation of a cheap mezzanine board onto the local PCI bus without coming to the VMEbus. The modern assortment of the PMC boards includes a wide spectrum of interfaces and devices of high performance.

In the module in question, the indicated possibility is used for organizing information exchange over the common information bus of the space ship.

The power consumption of the module V5A does not exceed 50 W, the board dimensions are 160×233 mm, the mass is 1 kg.

7. MAIN CHARACTERISTICS OF RADAR

1.	Mass	no more than 100 kg
2.	Consumed power	no more 2.5 kW
3.	Carrier frequency of radiation	95 GHz
4.	Diameter of antenna	2 m
5.	Antenna gain	63 dB
6.	Pulse duration of transmitter	0.8 μs
7.	Pulse recurrence rate	25 kHz
8.	Gain of receiving device	40 dB
9.	Noise temperature of receiving device with device of protection	around 200°K
10.	Dimension of observable objects	down to 1 mm
11.	Probability of detecting observable object flying over zone of 40000 m^2	no less than 0.95
12.	Quantity of facts of wrong object detections a day	no more than 0.05
13.	Root-mean-square error in measurement of range	no more than 9 m
14.	Root-mean-square error in measurement of angular coordinates	no more than 0.6 angular minutes
15.	Root-mean-square error in measurement of effective object cross-section of scattering	no more 1-to-2 dB
16.	Root-mean-square error in measurement of tangential and binormal velocity components	no more than 250 m/s
17.	Root-mean-square error in measurement of velocity component normal to space ship trajectory	no more 1000 m/s

8. CONCLUSION

In the present work, there have been done the following:

1. The principal possibility is shown of creating an on-board MMW radar for detecting and measuring coordinates of the space debris fragments of the order of 1 mm flying near a space ship over a zone of 40000 m^2 area.

2. It is shown that the transmitting block, as a most complex microwave element, is expedient to be realized on the basis of a vacuum device. The antenna should be realized in the form of an active phased array, and the receiving device is to be realized on the basis of solid-state transistors.

3. A scheme of computing devices construction has been proposed.

4. It is shown that the radar can be developed on the basis of the currently available elements.

5. The proposals on succession of performing the further work are presented in Appendix to the present report.

REFERENCES

1. A concept of creating low power space based radar to observe small-sized particles of space debris. (Interim Report, Part 1)
2. Technical Specifications for development of low power space based radar to observe millimeter fragments of space debris.
3. A. A. Tolkachev, V. V. Denisenko, A. V. Shihlov, and A. G. Shubov, High Gain Antenna Systems for Millimeter Wave Radar with Combined Electronical and Mechanical Beam Stering. IEEE International Symposium on Phased Array System and Technology, Boston, Massachusetts. October, 1996.
4. A. A. Tolkachev, V. P. Botavin, A. A. Kusmin, A. P. Pytsyk, V. A. Trushin. Radar Means for Detection and Tracking of Orbital Debris. Scientific Conference of the Russian Academy of Science 'Technodenous Space Debris Problems and Directions Research', Moscow, February, 1996.
5. M. D. Abouzahra and R. K. Avent. The 100 kw Millimetr-Wave Radar at the Kwajaleiu Atoll, IEEE Antennas and Propagation Magazine, Vol. 36, No. 2, April, 1994.
6. A Monolithic LNA for a band of 140 GHz. IEEE Microwave and Guided Wave Letters. – 1995, Vol. 5, No. 5, pp. 150-151.

APPENDIX

Proposals on succession of performing further work

1. Development, fabrication, and test of prototypes for main elements of the on-board radar:

– antenna module;
– transmitting-receiving block;
– master oscillator block;
– software (development and debugging with using a host computer);
– Deadline is the 2-nd quarter of 1999.

2. Development, fabrication, and test of radar equipment, including:
– antenna;
– block of information processing and control;
– debugging the radar software and equipment on a special setup with simulation of external radiolocation conditions and radar users.
– Deadline is the 2-nd quarter of 2000.

3. Study and justification of the choice of the space-based radar group configuration with evaluation of the expected efficiency.
– Deadline is the 2-nd quarter of 1998.